



Lawrence Berkeley Laboratory

UNIVERSITY OF CALIFORNIA

RECEIVED
LAWRENCE
BERKELEY LABORATORY

FEB 22 1982

LIBRARY AND
DOCUMENTS SECTION

ENERGY & ENVIRONMENT DIVISION

To be published as a chapter in *ATMOSPHERIC CHEMISTRY OF GASEOUS POLLUTANTS*, Ed. Stephen E. Schwartz, John Wiley & Sons, New York, NY, September 1982

THE ROLE OF CARBON PARTICLES IN ATMOSPHERIC CHEMISTRY

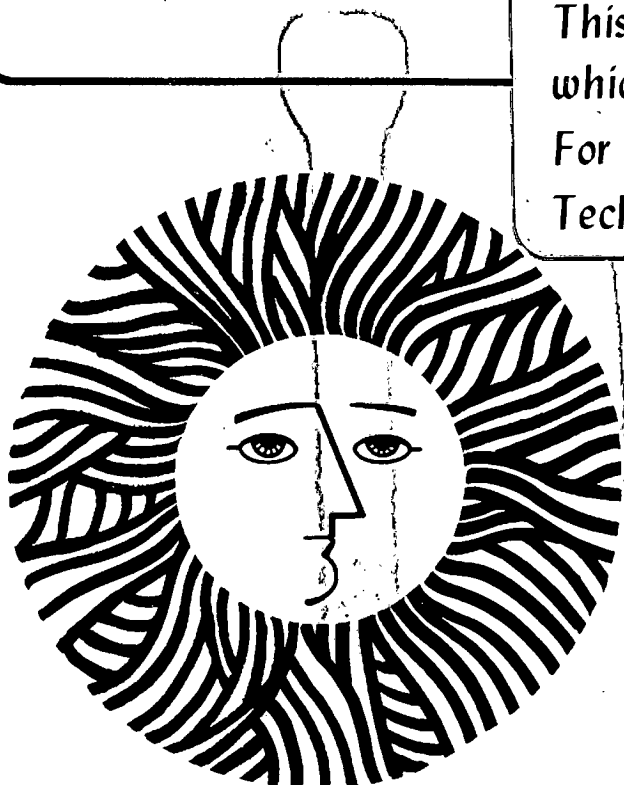
S.G. Chang and T. Novakov

January 1982

TWO-WEEK LOAN COPY

*This is a Library Circulating Copy
which may be borrowed for two weeks.*

*For a personal retention copy, call
Tech. Info. Division, Ext. 6782*



LBL-13879
c.2

DISCLAIMER

This document was prepared as an account of work sponsored by the United States Government. While this document is believed to contain correct information, neither the United States Government nor any agency thereof, nor the Regents of the University of California, nor any of their employees, makes any warranty, express or implied, or assumes any legal responsibility for the accuracy, completeness, or usefulness of any information, apparatus, product, or process disclosed, or represents that its use would not infringe privately owned rights. Reference herein to any specific commercial product, process, or service by its trade name, trademark, manufacturer, or otherwise, does not necessarily constitute or imply its endorsement, recommendation, or favoring by the United States Government or any agency thereof, or the Regents of the University of California. The views and opinions of authors expressed herein do not necessarily state or reflect those of the United States Government or any agency thereof or the Regents of the University of California.

THE ROLE OF CARBON PARTICLES IN ATMOSPHERIC CHEMISTRY*

S.G. Chang and T. Novakov
 Lawrence Berkeley Laboratory
 University of California
 Berkeley, California 94720

1. Introduction	1
2. Abundance	3
3. Composition	6
3.1. Bulk structure	6
3.2. Surface functional groups	7
4. Acidity	8
5. Chemical Activity	9
6. Catalytic Activity	16
6.1. Atmospheric reactions catalyzed by carbon particles	16
6.2. SO ₂ oxidation catalyzed by carbon particles	17
6.2.1. Dry mechanism	18
6.2.2. Wet mechanism	19
6.2.2.1. Kinetic studies	20
6.2.2.2. Relative importance of some wet SO ₂ oxidation mechanisms	24
Acknowledgment	27
References	28

1. INTRODUCTION

Carbonaceous particles in the atmosphere consist of two major components--graphitic or black carbon (sometimes referred to as elemental or free carbon) and organic material. The latter can be either directly emitted from sources (primary organics) or

*This work was supported by the Assistant Secretary for the Environment, Office of Health and Environmental Research, Pollutant Characterization and Safety Research Division of the U.S. Department of Energy under Contract No. W-7405-ENG-48 and by the National Science Foundation.

produced by atmospheric reactions from gaseous precursors (secondary organics). For the sake of clarity, we define soot as the total primary carbonaceous material, i.e., the sum of black carbon and primary organics. Black carbon is a chemically and catalytically active material and can be an effective carrier for other toxic air pollutants through their adsorptive capability. The chemical, adsorptive, and catalytic behaviors of black carbon particles depend very much on their crystalline structure, surface composition, and electronic properties. This paper discusses these properties and examines their relevance to atmospheric chemistry.

The assessment of the chemical role of black carbon in the atmosphere in general, and in photochemical environments such as Los Angeles in particular, had to start with an empirical assessment of the black carbon concentrations. While at one time the presence of soot in the atmosphere of industrial cities was obvious, it became less obvious in more recent times. Improvements in combustion technology and the use of better-grade fuels have led to the virtual elimination of visible smoke emissions. The emphasis of air pollution control thus shifted away from primary particulate emissions toward controlling gaseous emissions, especially in view of the newer concept of Los Angeles-type photochemical smog, which was believed to contain neither smoke nor fog. According to such a view, the haze over the Los Angeles Air Basin on polluted days is due almost entirely to the

photochemical conversion of certain invisible gases to light-scattering particles consisting of sulfates, nitrates, and secondary organics but almost no soot. The results of our studies, as shown below, have clearly demonstrated that soot is ubiquitous not only in urban atmospheres but also in remote regions such as the Arctic (Rosen et al., 1981). Los Angeles, with its abundant coastal fog, contains both components of London-type fog--smoke (or soot) and fog.

2. ABUNDANCE

The methodology that we adopted involved systematic measurements of the ratio of black carbon to total carbon for a large number of samples collected directly from sources, source-dominated environments, and well-aged ambient air (24-hour samples) (Hansen et al., 1980). The ambient samples were collected in areas with widely different atmospheric chemical characteristics (e.g., degree of photochemical activity, source composition, geographic location). Measurements of this ratio from a number of source samples give insights into the relative black to total carbon ratio of primary emissions and the source variabilities. Secondary material will not contain the black component but will increase the total mass of carbon and therefore reduce the black to total carbon fraction. That is, under high photochemical conditions one would expect this ratio to be significantly smaller than under conditions obviously heavily influenced by sources.

Because of the large number of samples that had to be analyzed, a fast-throughput optical attenuation method (Rosen et al., 1980) was used for determining black carbon. The validity of the optical attenuation method was checked by performing Raman spectroscopic (Rosen et al., 1978) and opto-acoustic (Yasa et al., 1978) measurements on some of the ambient and source samples. Total particulate carbon was determined by a combustion method.

The optical attenuation method compares the transmission of a 633-nm He-Ne laser beam through a loaded filter relative to that of a blank filter. The relationship between the optical attenuation and the black carbon content can be written as:

$$[C_{\text{black}}] = \frac{1}{K} \times \text{ATN}, \quad (1)$$

where $\text{ATN} = -100 \ln(I/I_0)$. I and I_0 are the transmitted light intensities for the loaded filter and for the filter blank.

Besides the black carbon, particulate material also contains organic material which is not optically absorbing. The total amount of particulate carbon is then

$$[C_{\text{tot}}] = [C_{\text{black}}] + [C_{\text{org}}]. \quad (2)$$

We define specific attenuation (σ) as the attenuation per unit mass of total carbon:

$$\sigma \equiv \frac{\text{ATN}}{[\text{C}_{\text{tot}}]} = K \times \frac{[\text{C}_{\text{black}}]}{[\text{C}_{\text{tot}}]} \quad (3)$$

The determination of specific attenuation therefore gives an estimate of black carbon as a fraction of total carbon.

The proportionality constant K , which is equal to the specific attenuation of black carbon alone, was recently shown to have an average value of 20 (Hansen et al., 1980). In principle the percentage of soot (i.e., primary carbonaceous material) in ambient particles can be determined from the ratio of ambient specific attenuation and an average specific attenuation of major primary sources (Novakov, 1981):

$$\frac{[\text{Soot}]}{C} = \frac{\sigma_{\text{ambient}}}{\sigma_{\text{source}}} \quad (4)$$

Table 1 lists the average and extreme values of specific attenuation and the black carbon fraction of a number of source samples.

The percentage of soot in ambient carbonaceous particulates can be estimated by comparing the σ of sources with that of ambient samples. The fraction of soot is given in Eq. 4. Table 2 lists the mean specific attenuation of ambient samples (weekends excluded) in order of decreasing σ and soot fractions obtained by using Eq. 4 and $\sigma_{\text{source}} = 5.85$.

Table 1. Specific attenuation (σ) and black carbon (BC) (% of total C) of source samples.

Source	Number						
	of samples	Average		Highest		Lowest	
		σ	% BC	σ	% BC	σ	% BC
Parking garage	12	5.4	27	7.7	39	2.25	11
Diesel	6	5.6	28	5.7	29	3.5	18
Scooter	9	5.1	26	6.1	31	4.2	21
Tunnel	63	6.3	32	12.5	63	3.7	19
Natural gas	6	2.6	13	3.3	17	1.9	10
Garage and tunnel		5.85	29				

Table 2. Mean specific attenuation of ambient samples.

Site	Number		Standard deviation	Soot (%)
	of samples	$\bar{\sigma}$		
New York	211	5.69	1.34	97
Gaithersburg	155	4.72	1.51	81
Argonne	221	4.35	1.64	74
Berkeley	513	4.28	1.47	73
Anaheim	444	3.99	1.71	68
Fremont	461	3.74	1.25	64
Denver	42	3.47	1.49	59

Based on this estimate, the New York City carbonaceous aerosol is essentially primary soot. A different value of σ_{source} would certainly change the estimated soot percentage. However, New York City's average soot content would nevertheless remain the highest, irrespective of the actual numerical value of σ_{source} . It is logical that samples from this location have the highest soot content because the site represents a heavily traveled street canyon. Fremont and Anaheim samples have the smallest soot content on the average, as might be expected, because both sites represent receptor sites.

These results demonstrate that black carbon is certainly a major fraction of ambient particulate carbon at all locations studied. These findings also suggest that in the atmosphere there is a catalytically active material which is present in high concentrations so that the assessment of its role in heterogeneous atmospheric chemistry is warranted.

3. COMPOSITION

3.1. Bulk Structure

The diameter of black carbon particles varies from 50 Å or even smaller to several thousand Angstroms. The results of x-ray diffraction (Hofmann and Wilm, 1936) have shown that each particle is made up of a large number of crystallites 20 to 30 Å in diameter. Each crystallite consists of several carbon layers with a graphitic hexagonal structure, having defects, dislocations, and discontinuities

in the layer planes, and thus containing high concentrations of unpaired electrons which constitute the active sites. Carbon atoms located at these sites show strong tendencies to react with other molecules because of residual valencies. During particle formation, interactions of air, water, flue gas, etc., with carbon particles occur, resulting in the incorporation of 5-15% oxygen, 1-3% hydrogen, and traces of nitrogen into the structure.

3.2. Surface Functional Groups

Nearly every type of oxygen-containing functional group known in organic chemistry has been postulated to exist on the carbon surface (Figure 1). The functional groups most often suggested are carboxyl groups, phenolic hydroxyl groups, and quinone carbonyl groups (Garten and Weiss, 1957; Boehm, 1966; Coughlin and Ezra, 1968; Puri, 1970, 1966; Smith, 1959; Zary'yanz et al., 1967). Less often suggested are ether, peroxide, and ester groups in the forms of normal and fluorescein-like lactones (Garten et al., 1957), carboxylic acid anhydrides (Boehm et al., 1964), and cyclic peroxide (Puri, 1962). The relative amounts of these complexes and their structure depends on the thermal history of carbon particles (Hart et al., 1967; Laine et al., 1963; Palmer and Cullis, 1965; Weller and Young, 1948). Little is known about the structure of surface nitrogen species, although the capability of fixation of nitrogen (Emmett, 1948) in carbon particles and the promoting effect of the catalytic activity

of nitrogenous carbon (Larsen and Walton, 1940) have been observed. Therefore, black carbon particles may be regarded as a complex three-dimensional organic polymer with the capability of transferring electrons, rather than merely as an amorphous form of elemental carbon.

4. ACIDITY

Depending on the thermal history, black carbon particles may possess either acidic or basic character. Because of this property, soot may influence the pH of atmospheric water droplets (Chang and Novakov, 1975). It has been shown that activation of elemental carbon by exposure to O_2 at temperatures between 200 and 400°C produces an acidic type. By contrast, activation of carbon at high temperatures either in pure CO_2 or under vacuum, followed by exposure to oxygen at room temperature, results in a basic type.

The acidic character can be explained by the dissociation of acidic oxygen functional groups such as carboxyl and hydroxyl in solution. The nature of the basic character has been a topic of considerable discussion and controversy (Schilow, Schatunowskja, and Tshmutow, 1930; Rivin, 1963; Frumkin et al., 1931; Steenberg, 1944; Mattson and Mark, 1971). The idea of the presence of basic sites in the form of surface oxides has been proposed by Schilow, Schatunowskja, and Tschmutow (1930), among others, to account for the chemisorption of acids. The latter suggested that the oxides were in the form of a chromene-like structure after neutralization with acid, which would result in the formation of

carbonium ion. The presence of carbonium cationic sites on the surface of acid-treated carbon was confirmed by Rivin (1963), but it could not be established whether the basic sites are due to the presence of the chromene-like surface oxides or the inherent property of the polynuclear aromatic structures of the carbon particles. Frumkin et al. (1931) proposed an electrochemical theory in which the adsorption of the acids by carbon is determined by the electrical potential at the carbon solution interface and by the capacity of the double layer. According to Steenberg (1944), adsorption of acids involved primary adsorption of protons by physical force and secondary adsorption of anions in the diffuse double layer. On the contrary, Mattson and Mark (1971) attributed the neutralization of acids at high acid concentrations to the primary adsorption of the anions and secondary adsorption of the protons.

5. CHEMICAL ACTIVITY

We have investigated the reaction between black carbon particles and NH_3 in both an oxidizing and a reducing atmosphere. The first set of experiments involves the exposure of combustion-produced soot with NH_3 in air. The nature of nitrogen species thus formed was studied with the aid of ESCA. Soot particles for these experiments were generated by a premixed propane-oxygen flame. The exposure of soot particles to NH_3 was done under two different experimental conditions: in a static regime, with propane soot precollected on a silver membrane filter subsequently exposed to the reactant gas

at ambient temperature; and in a flow system, by introducing the reactant gas downstream from the propane-oxygen flame, i.e., while the soot particles are still at high temperature.

ESCA spectra of the nitrogen (1s) region of soot samples prepared in these ways are shown in Figures 2 and 3. Interaction of NH_3 with "cold" soot particles can result in ammonium-like species (Figure 2). However, as seen from Figure 3, NH_3 interacting with "hot" soot particles produces species with ESCA peaks of binding energies designated as N_x species. Ammonium in these samples is probably produced on soot particles after they have been collected on the filter and cooled down.

Using ESCA to analyze ambient particulates, Novakov et al. (1972) have observed, in addition to commonly occurring nitrate and ammonium, two reduced nitrogen species with N(1s) binding energy corresponding to N_x surface species produced under laboratory conditions. Chemical equivalency of ambient and synthetic N_x species is demonstrated by their thermal behavior. The experimental procedure is to measure ESCA spectra at gradually increasing sample temperatures. The results of such measurements for one ambient particulate sample, collected in Pomona, California, during a moderate smog episode (24 October 1972) and for a sample prepared by NH_3 -hot soot interaction are shown in Figures 4 and 5.

The spectrum of the ambient sample (Figure 4) at 25°C shows the presence of NO_3^- , NH_4^+ , and N_x . At 80°C the entire nitrate

peak is lost, accompanied with a similar loss in ammonium peak intensity. The shaded portion of the ammonium peak in the 25°C spectrum represents the ammonium fraction volatilized between 25 and 80°C. It appears therefore that the nitrate in this sample is mainly in the form of ammonium nitrate. At 150°C the only nitrogen species remaining is N_x . The ammonium fraction still present at 80°C but absent at 150°C is associated with some ammonium compound more stable than NH_4NO_3 , possibly ammonium sulfate. At 250°C the appearance of another peak, labeled N_x' , is seen. This peak continues to increase at 350°C. The total peak areas of spectra recorded at 150, 250, and 350°C remain constant, indicating that the N_x component is transformed into N_x' by heating in vacuum.

N_x species produced by surface reactions of hot soot with NH_3 have the same kind of temperature dependence as the ambient samples. This is illustrated in Figure 5. The spectrum taken at room temperature shows that most nitrogen species in this sample are of the N_x type. Heating the sample in vacuum to 150°C does not influence the line shape or intensity. At 250°C, however, the formation of N_x' is evident. Further transformation of N_x to N_x' occurred at 350°C.

Both ambient and synthetic N_x' species will remain unaltered even if the temperature is lowered back to room temperature if the sample remains in vacuum. However, if the sample is taken out of vacuum and exposed to moisture, N_x' will be transformed back to the original N_x compound. It can be concluded that N_x' species are

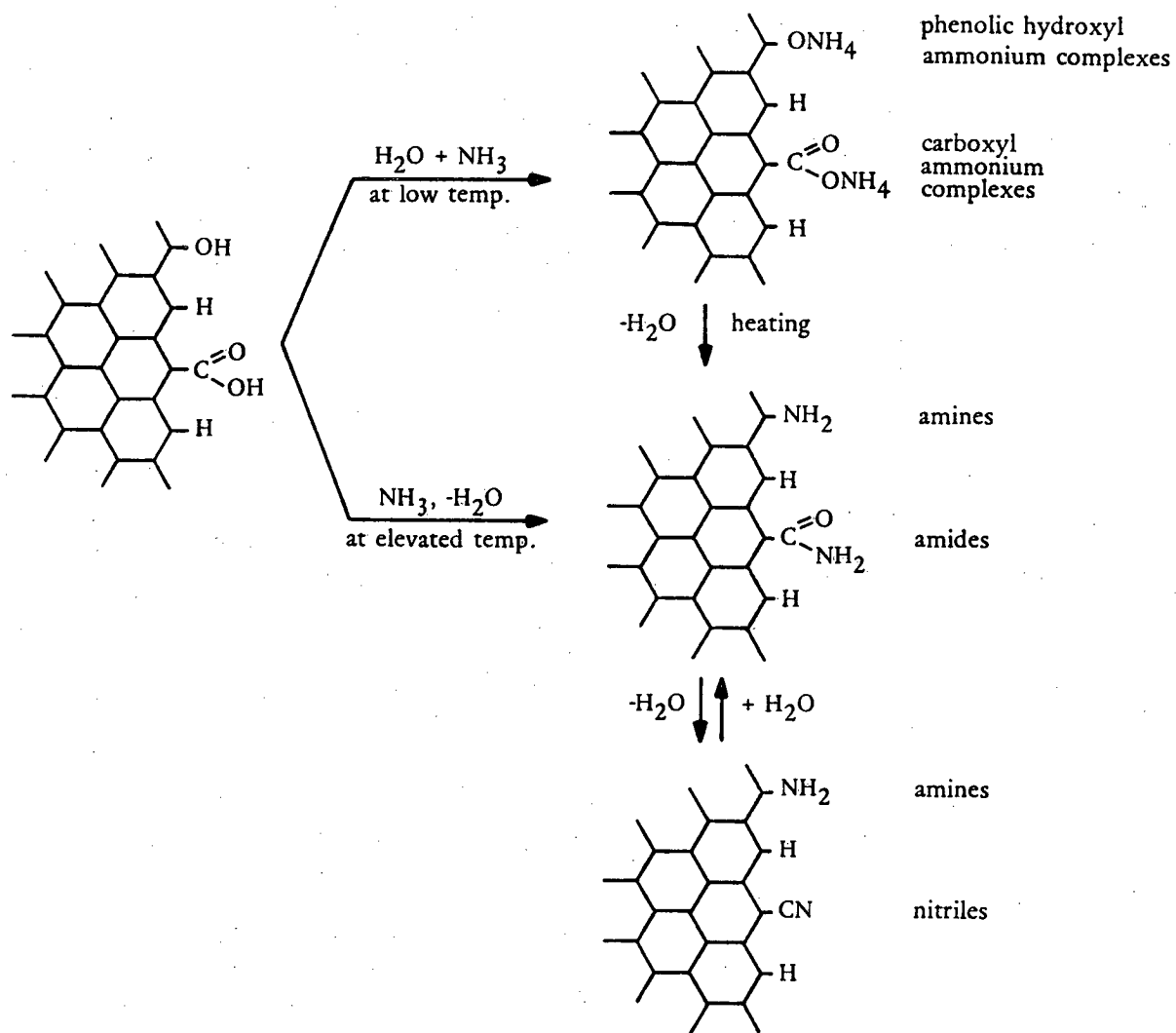
produced by dehydration of N_x .

The outlined results indicate that the thermal behavior of nitrogen species of the N_x and N_x' type observed in ambient pollution particulates is identical to the reduced nitrogen species produced by reactions at elevated temperature of ammonia with finely divided carbon or soot.

Based on these experimental results, N_x was assigned to a mixture of amines and amides, and N_x' to nitrile. Since prior to the interaction with NH_3 , the soot particle surface was in contact with air and flue gas, it therefore should be covered with surface oxygen complexes. By using the most often-mentioned surface oxygen-carbon functional groups (i.e., carboxyl groups and phenolic hydroxyl groups) and in analogy with organic chemistry, we can describe some possible reactions of NH_3 and soot leading to the formation of amides, amines, nitriles, and ammonium-salt-like compounds associated with the black carbon component of soot particles.

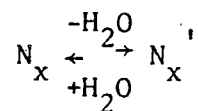
At low temperatures black carbon covered with surface carboxyl or phenolic groups may act as a Bronsted acid when interacting with NH_3 . Carboxyl ammonium or phenolic ammonium salts will be formed as the result of proton exchange. Ammonia may also be physically adsorbed by hydrogen bonding to surface OH or COOH groups. At elevated temperatures the carboxyl group carbon is electrophilic and has the tendency to accept an electron pair from the basic species in the process of coordination. The nucleophilic substitution reaction of NH_3 with carboxylic acid yields an amide which may

dehydrate and become a nitrile upon further heating. Carboxyl and phenolic hydroxyl ammonium salts may dehydrate at elevated temperature to produce amides and/or nitriles and amines respectively.



XBL-7410-1814

The photoelectron spectroscopic results indicate that the amides and amines correspond to the N_x species. These appear as broad peaks indicating the presence of more than one chemical species. Nitriles formed from amides by dehydration on heating correspond to the N_x' species. We have established the reversibility of the



process. The carboxyl ammonium and phenolic hydroxyl ammonium salts produced by NH_3 chemisorption correspond to the volatile ambient ammonium species.

We have studied the stability of ambient particulate nitrogen in water by combining ESCA measurements with determination of total nitrogen by proton activation (Gundel et al., 1979). Our results with samples from several locations (Berkeley, Los Angeles, and St. Louis) indicate that 1) a large fraction of N_x (85%) originally present in ambient particulate matter can be removed by water extraction; and 2) more NH_4^+ appears in the extract than was present on the untreated sample and less N_x appears in the extract than was present on the untreated sample. The N_x deficiency in the extract matches the surplus in NH_4^+ . The former behavior could be attributed to water-soluble stoichiometric compounds such as amines and surface species such as amides and nitrile which can undergo hydrolysis.

The latter could be attributed to the hydrolysis of amide and nitrile groups. These behaviors may be responsible for the disagreement of chemical composition in black episodes with those predicted from the equilibrium phase diagram as constructed by Brosset (1980).

The other set of experiments (Novakov and Chang, 1977) involves the grinding of a purified grade POCO graphite in NH_3 in the absence of air at room temperature. The concentration of nitrogen with respect to carbon was determined by ESCA. The information on the structure of surface nitrogen species was obtained with the aid of Fourier transform infrared spectroscopy. To help in the assignment of vibrational frequencies, infrared spectra of graphite particles after reaction with deuterated ammonia were also obtained.

The grinding reduced particle sizes and creates fresh surfaces. Surface carbon atoms of graphite particles show a strong chemical reactivity because of unsaturation in valency. Figures 6a and 6c show infrared spectra of the graphite particles after extensive grinding in an atmosphere of NH_3 and ND_3 , with expansions of these spectra in Figures 6b and 6d. These infrared spectra suggest the occurrence of dissociative chemisorption of NH_3 on the carbon particle surface. Vibrational frequencies associated with the surface groups C-NH_2 , C=N-H , $\text{C}\equiv\text{N}$, and C-H are observed in Figures 6a and 6b. The isotope shifts shown in Figures 6c and 6d support these assignments. Surface CNH_2 groups give rise to two bands near 3400 cm^{-1} that are attributed to symmetric and antisymmetric N-H stretching modes. These two bands should shift to 2500 cm^{-1} for CND_2 . This shift is

shown in Figures 6c and 6d. A NH_2 bending mode near 1580 cm^{-1} should shift to about 1200 cm^{-1} for the ND_2 groups. However, a strong band due to the $k=0, E_{2g}$ phonon mode of the graphite lattice (Tuinstra and Koenig, 1970) and/or a vibrational mode of the aromatic structure of graphite (Friedel and Hofer, 1970) also occurs at about 1580 cm^{-1} . Likewise, the C-N stretching mode vibrates at approximately 1200 cm^{-1} and appears in both the C- NH_2 and the C- ND_2 surface groups.

We have detected surface nitrogen groups indicating the dissociation of more than one bond in a molecule of ammonia. A band between 1600 and 1700 cm^{-1} could be assigned to immines (C=NH and C=N-C), a weak band at 2300 cm^{-1} to nitrile (C \equiv N), and one at 2180 cm^{-1} to isocyanide ($-\text{N}^+ \equiv \text{C}^-$).

The evidence of the dissociative chemisorption of ammonia on carbon particle surfaces is also supported by the appearance of the C-D stretching band at 2050 cm^{-1} . The assignment of the C-H stretching is ambiguous because the C-H stretching is near 2900 cm^{-1} where a vibrational band appears on both NH_3 and ND_3 samples. This band could be the overtone and/or combination bands resulting from the strong absorption band between 1300 and 1600 cm^{-1} . There is also a band, possibly of the same nature, at 2700 cm^{-1} in both samples.

6. CATALYTIC ACTIVITY

6.1. Atmospheric Reactions Catalyzed by Carbon Particles

Black carbon particles are effective catalysts (Coughlin, 1969) for many different types of reactions including oxidation-reduction,

halogenation, hydrogenation-dehydrogenation, dehydration, polymerization, and isomerization. Table 3 lists a few reactions catalyzed by carbon that could have direct bearing on atmospheric chemistry.

It is difficult to assess the importance of all these reactions in the atmosphere at this time because useful rate equations have not been determined. We have recently performed a study (Chang et al., 1979; Brodzinsky et al., 1980) on the kinetics and mechanism for the catalytic oxidation of SO_2 on carbon in aqueous suspensions and have obtained a rate equation applicable to atmospheric conditions.

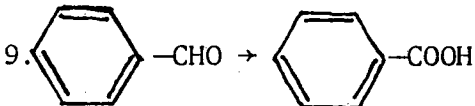
6.2. SO_2 Oxidation Catalyzed by Carbon Particles

Novakov et al. (1974) used photoelectron spectroscopy (ESCA) to study the oxidation of SO_2 on carbon particles produced by a propane flame. They found that under some conditions, a significant amount of sulfate can be produced by the catalytic action of carbon particles.

Although these early experiments were qualitative, it was nevertheless possible to conclude the following:

1. The reaction product is in a 6+ oxidation state (i.e., sulfate).
2. Soot-catalyzed oxidation of SO_2 is more efficient at a higher humidity.
3. The oxygen in air plays an important role in SO_2 oxidation.
4. Black carbon-catalyzed oxidation exhibits a saturation effect.

Table 3. Some reactions catalyzed by carbon.

Reactions	References
1. $\text{SO}_2 + 1/2 \text{O}_2 \rightarrow \text{SO}_3$	Novakov et al. (1974), Chang et al. (1979), Brodzinsky et al. (1980), Chang et al. (1981)
2. $\text{SO}_2 + \text{NO}_2 \rightarrow \text{SO}_3 + \text{NO}$	Cofer et al. (1980), Britton and Clarke (1980)
3. $\text{SO}_2 + \text{O}_3 \rightarrow \text{SO}_3 + \text{O}_2$	Cofer et al. (1981)
4. $\text{NO} + 1/2 \text{O}_2 \rightarrow \text{NO}_2$	Rao and Hougen (1952)
5. $2\text{H}_2\text{O}_2 \rightarrow 2\text{H}_2\text{O} + \text{O}_2$	Bente and Walton (1943)
6. $\text{CO} + \text{Cl}_2 \rightarrow \text{COCl}_2$	Dulou (1945)
7. $\text{SO}_2 + \text{Cl}_2 \rightarrow \text{SO}_2\text{Cl}_2$	Dulou (1945)
8. $\text{HCOOH} \begin{cases} \rightarrow \text{H}_2\text{O} + \text{CO} \\ \rightarrow \text{H}_2 + \text{CO}_2 \end{cases}$	Stumpp (1965)
9. 	Gundel (1979)
10. <u>Hydroquinone \rightarrow quinhydrone \rightarrow quinone</u>	Bente and Walton (1943)

5. SO_2 can be oxidized on other types of graphitic carbonaceous particles, such as ground graphite particles and activated carbon.

Results from the experiments with combustion-produced soot particles are essentially similar to those obtained for activated carbon by Davtyan and Tkach (1961) and Siedlewski (1965).

Soot-catalyzed SO_2 oxidation can proceed by two mechanisms: a "dry" mechanism, in the presence of water, and a "wet" mechanism, when the soot particles are covered by a liquid water layer. The wet mechanism is much more efficient than the dry and is applicable to situations in plumes, clouds, fogs, and the ambient atmosphere when the aerosol particles are covered with a liquid water layer. The dry mechanism is expected to operate in stacks or under conditions of low relative humidity.

6.2.1. Dry mechanism

A description of the dry mechanism was given by Yamamoto et al. (1972), who studied the reaction kinetics on dry activated carbon in the presence of O_2 and H_2O vapor. The rate of reaction was found to be first order with respect to SO_2 , provided that the concentration of SO_2 was less than 0.01%, and depended on the square root of the concentration of O_2 and H_2O vapor. The activation energy was found to vary from -4 to -7 kcal/mole between 70°C and 150°C, depending on the origin of the activated carbon. Initially the reaction occurs on the surface of both micropores and macropores, and the rate is

constant for a given activated carbon until the amount of accumulated H_2SO_4 reaches about 10% by weight of the carbon. Beyond that amount, the rate gradually decreases with the reaction time until the micropore volume is filled up by H_2SO_4 . The reaction continues only on the macropores at a constant, but much slower, rate.

According to Yamamoto et al. (1972), a rate expression (until the amount of H_2SO_4 formed reaches 10% by weight of the carbon) for activated carbon used can be written as follows:

$$\frac{d[H_2SO_4]}{dt} = [C_x][SO_2][O_2]^{0.5}[H_2O]^{0.5}(k_{\text{micro}} + k_{\text{macro}})e^{\frac{-E_a}{RT}},$$

where t is time, $[C_x]$ is the concentration of carbon, k_{micro} and k_{macro} are the rate constants on the surface of the micropores and macropores, E_a is the activation energy, R is the universal gas constant, and T is absolute temperature.

The dry mechanism is relatively inefficient because the reaction product remains on the carbon surface and acts as the catalyst poison.

6.2.2. Wet mechanism

The situation is entirely different when soot (or black carbon) is covered with a layer of liquid water and the catalytic oxidation occurs at the solid-liquid interface: there is constant regeneration of active sites because the reaction product is soluble in water and therefore leaves the soot surface. Such reactions were studied in detail by Chang et al. (1979, 1981) and Brodzinsky et al. (1980),

who used both combustion soots and activated carbons.

6.2.2.1. Kinetic studies

The reaction was studied by batch (flask) experiments, from which a rate law was derived. This rate law has been confirmed by fog chamber studies (Benner, 1980). The flask experiments were performed using suspensions of commercially available activated carbons as well as suspensions of combustion-produced soots.

Figure 7 shows the typical reaction curves of the oxidation of S(IV) in aqueous suspensions of soot particles collected from acetylene and natural gas flames. The reaction occurs in two steps. The initial disappearance of S(IV) is so fast that its rate could not be followed by the analytical techniques used. The second step is characterized by a much slower reduction of S(IV). The results obtained with these combustion-produced soots were reproduced (Figure 8) by suspensions of similar concentrations of one of the commercially available activated carbons (Nuchar C-190, a trademark of West Virginia Pulp and Paper Co.). Figure 8 also shows a mass balance between the S(IV) consumed and the sulfate produced. At a constant temperature, the amount of S(IV) oxidized by the rapid first step process was found to be proportional to the carbon particle concentration.

The reaction of the second step has the following characteristics:

1. The reaction rate is independent of pH ($\text{pH} < 7.6$), and

therefore $\text{SO}_2 \cdot \text{H}_2\text{O}$, HSO_3^- , and SO_3^{2-} are indistinguishable in terms of oxidation on the carbon surfaces.

2. The reaction is first order with respect to the concentration of carbon particles.

3. The activation energy of the reaction is ~ 8.5 kcal/mole, being slightly different for different carbons.

4. The reaction rate has a complex dependence on the concentration of S(IV), ranging between a second and zeroth order reaction as the S(IV) concentration increases.

5. The reaction rate has a complex dependence on the concentration of dissolved O_2 , with the order of reaction between zeroth and first.

Figure 9 shows the effective rate of reaction (normalized carbon concentration, room temperature--20°C, and air) as a function of the sulfurous acid concentration for the activated carbons studied (see also Table 4). From the Nuchar C-190 curve, the rate of reaction is second order with respect to S(IV) below 10^{-7} M, moves through a first order reaction around 5×10^{-6} M, and becomes independent of S(IV) concentrations above 10^{-4} M. The other curves are seen to be similar in their behavior.

Based on the experimental results, we propose the following reaction mechanism

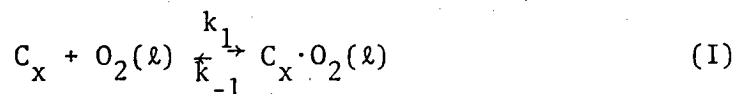
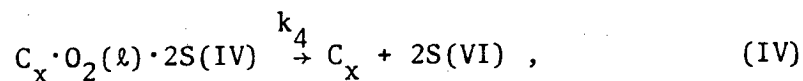
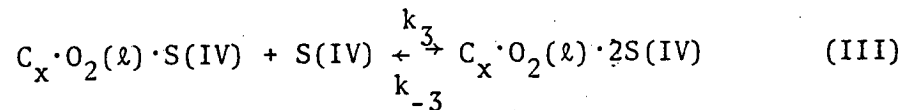
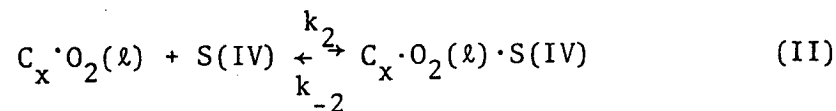


Table 4. Summary of kinetic data for the catalytic oxidation of SO_2 by various elemental carbon particles in aqueous suspension.

Reaction rate equation:

$$\frac{d[\text{SO}_4^{-2}]}{dt} = A e^{\frac{-E_a}{RT}} [\text{C}_x] \left\{ \frac{K_1 [\text{O}_2]}{1 + K_1 [\text{O}_2]} \right\} \left\{ \frac{\alpha [\text{S(IV)}]^2}{1 + \beta [\text{S(IV)}] + \alpha [\text{S(IV)}]^2} \right\}$$

Kinetic data	Elemental carbon	Nuchar	Nuchar	
		C-190 (WESVACO)	SN (WESVACO)	Aktivkohle (MERCK)
A (moles/g-sec)		0.874	0.158	2.473
E_a (kcal/mole)		8.8	8.1	8.8
K_1 (l/mole)		2.103×10^3	7.427×10^3	4.372×10^3
α (l ² /mole ²)		2.404×10^{12}	4.915×10^8	9.519×10^{11}
β (l/mole)		1.219×10^7	2.956×10^5	3.738×10^7



where C_x = soot, $O_2(\ell)$ = dissolved oxygen molecule, $S(\text{IV})$ = sulfite species, and $S(\text{VI})$ = sulfate species.

Equation (I) indicates that dissolved oxygen is adsorbed on the soot particle surface to form an activated complex. This adsorbed oxygen complex then oxidizes the $S(\text{IV})$ to form sulfate according to Equations (II)-(IV). If one assumes that the reaction follows the condition of Langmuir adsorption equilibrium (Clark, 1970), the rate of acid formation is

$$\frac{d[S(\text{VI})]}{dt} = 2k_4 [C_x] \left(\frac{K_1 [O_2]}{1 + K_1 [O_2]} \right) \left(\frac{K_2 [S(\text{IV})]}{1 + K_2 [S(\text{IV})]} \right) \left(\frac{K_3 [S(\text{IV})]}{1 + K_3 [S(\text{IV})]} \right) \quad (5)$$

where $K_1 = k_1/k_{-1}$, $K_2 = k_2/k_{-2}$, $K_3 = k_3/k_{-3}$.

The experimental results yield the following rate law for this reaction:

$$\frac{d[S(\text{VI})]}{dt} = k [C_x] \left(\frac{K [O_2]}{1 + K_1 [O_2]} \right) f[S(\text{IV})] \quad (6)$$

$$\text{where } f[\text{S(IV)}] = \left(\frac{\alpha[\text{S(IV)}]^2}{1 + \beta[\text{S(IV)}] + \alpha[\text{S(IV)}]^2} \right).$$

$[\text{C}_x]$ = grams of carbon particles per liter,

$[\text{O}_2]$ = moles of dissolved oxygen per liter, and

$[\text{S(IV)}]$ = total moles of S(IV) per liter.

For Nuchar C-190 the following constants were determined: $k = 0.874 e^{-4428/T}$ moles/g·sec ($T = \text{°K}$); $K_1 = 2.103 \times 10^3$ L/mole, $\alpha = 2.404 \times 10^{12}$ L²/mole², and $\beta = 1.219 \times 10^7$ L/mole.

The dependence of the rate of formation of sulfate on the partial pressure of SO_2 (P_{SO_2}) in the atmosphere can be obtained from Eq. 6. Because the effect of P_{SO_2} on the rate is contained in $f[\text{S(IV)}]$, we illustrate the relationship of $f[\text{S(IV)}]$ with P_{SO_2} and pH of the aqueous droplets as shown in Figures 10 and 11. $f[\text{S(IV)}]$, or the rate of production of sulfate (because the rate is linearly proportional to $f[\text{S(IV)}]$), decreases as the pH decreases at a given P_{SO_2} . The magnitude of $f[\text{S(IV)}]$'s changing per unit pH change is much larger at a lower P_{SO_2} . Also $f[\text{S(IV)}]$ (or the rate) depends only slightly on P_{SO_2} under most atmospheric conditions when P_{SO_2} is between 1 and 10 ppb and the pH ranges between 5 and 6. $f[\text{S(IV)}]$ increases only 1/10 and twofold respectively at pH of 6 and 5 when P_{SO_2} increases from 1 to 10 ppb. However, $f[\text{S(IV)}]$ depends strongly on P_{SO_2} when the pH is low.

The catalytic oxidation of sulfurous acid on carbon particles of different origins shows the same kinetic behavior. However, the rate constants of several different types of carbon particles were

studied and found to differ from type to type. In principle, the reaction rate should be proportional to the concentration of active sites on the carbon particles, rather than to the concentration of carbon particles. The number of active sites per unit mass of carbon particles is different from type to type and is not necessarily proportional to the surface area. Sidelewski (1965) has shown, by means of the electron paramagnetic resonance method, that free electrons on carbon particles can serve as active centers for the adsorption of oxygen molecules and for the oxidation of SO_2 . The concentration of free electrons is related to the origin and thermal history of the carbon particles.

It is therefore impractical to formulate a generally applicable rate constant for atmospheric soot particles because these particles may arise from the combustion of different types of fossil fuel under different combustion conditions and thus possess a different catalytic activity.

6.2.2.2. Relative importance of some wet SO_2 oxidation mechanisms

We have carried out a box-type calculation (Chang et al., 1979, 1981) to compare the relative importance of sulfate production mechanisms by black carbon particles with other mechanisms involving liquid water. The systems considered in the batch reactor include the SO_2 - CO_2 - $\text{H}_2\text{O}(\ell)$ -air and any of the oxidizing agents such as O_2 , O_3 , HNO_2 , or catalysts such as Fe^{+++} , Mn^{++} , and black carbon. The role of NH_3 is investigated in these reactions. The kinetic results

of Chang et al. (1981) and Oblath et al. (1980), Beilke et al. (1975), Erickson et al. (1977), Freiberg (1975), and Matteson et al. (1969) for nitrous acid, oxygen, ozone, iron, and manganese systems respectively were used in this calculation.

All the oxidation mechanisms considered except Mn^{++} are pH dependent. Most of these mechanisms have lower oxidation rates at a lower pH, but some are more sensitive to the change in pH than others. The HNO_2 mechanism shows a larger oxidation rate when the solution is more acidic, however. The following initial conditions were used in the calculation: liquid water, 0.05 g/m^3 ; SO_2 , 0.01 ppm; O_3 , 0.05 ppm; and CO_2 , 0.000311 atm. Concentrations of particulate Fe and Mn of 250 ng/m^3 and 20 ng/m^3 respectively were assumed. However, only 0.13% of the total iron and 0.25% of the manganese are water soluble, according to Gordon et al. (1975). The concentrations of black carbon and HNO_2 were taken as $10 \text{ } \mu\text{g/m}^3$ and 8 ppb respectively. The latter corresponds to 25 ppb of NO and 50 ppb of NO_2 at equilibrium conditions. For NH_3 a concentration of 5 ppb was used, which is higher than the highest equilibrium partial pressure of NH_3 over the United States as calculated by Lau and Charlson (1977). Tables 5 and 6 list the equilibrium equations and oxidation rate equations used for this comparative study.

The following assumptions were made in the calculations:

1. The size of liquid water drops suspended inside the box is so small that the absorption rate of gaseous species (SO_2 , NH_3 ,

Table 5. Chemical equilibrium constants at 25°C.^a

$\text{H}_2\text{O} \rightleftharpoons \text{H}^+ + \text{OH}^-$	$K_2 = 1.008 \times 10^{-14}$
$\text{CO}_2(\text{g}) + \text{H}_2\text{O}(\text{l}) \rightleftharpoons \text{CO}_2 \cdot \text{H}_2\text{O}$	$H_c = 3.4 \times 10^{-2}$
$\text{CO}_2 \cdot \text{H}_2\text{O} \rightleftharpoons \text{CO}_3^{-2} + \text{H}^+$	$K_{1c} = 4.45 \times 10^{-7}$
$\text{HCO}_3^- \rightleftharpoons \text{HCO}_3^- + \text{H}^+$	$K_{2c} = 4.68 \times 10^{-11}$
$\text{NH}_3(\text{g}) + \text{H}_2\text{O}(\text{l}) \rightleftharpoons \text{NH}_3 \cdot \text{H}_2\text{O}$	$H_a = 57$
$\text{NH}_3 \cdot \text{H}_2\text{O} \rightleftharpoons \text{NH}_4^+ + \text{OH}^-$	$K_a = 1.774 \times 10^{-5}$
$\text{SO}_2(\text{g}) + \text{H}_2\text{O}(\text{l}) \rightleftharpoons \text{SO}_2 \cdot \text{H}_2\text{O}$	$H_s = 1.24$
$\text{SO}_2 \cdot \text{H}_2\text{O} \rightleftharpoons \text{HSO}_3^- + \text{H}^+$	$K_{1s} = 1.7 \times 10^{-2}$
$\text{HSO}_3^- \rightleftharpoons \text{SO}_3^{-2} + \text{H}^+$	$K_{2s} = 6.24 \times 10^{-8}$
$\text{HSO}_4^- \rightleftharpoons \text{H}^+ + \text{SO}_4^{-2}$	$K_{3s} = 1.2 \times 10^{-2}$
$\text{HNO}_2(\text{g}) + \text{H}_2\text{O} \rightleftharpoons \text{HNO}_2 \cdot \text{H}_2\text{O}$	$H_N = 49$
$\text{HNO}_2 \cdot \text{H}_2\text{O} \rightleftharpoons \text{H}^+ + \text{NO}_2^-$	$K_N = 5.1 \times 10^{-4}$

Table 5 continued



^aConcentrations in moles/l and gas pressure in atm.

Table 6. Rate of SO₂ oxidation by various mechanisms in aqueous droplets.

Mechanism	Reaction rate law ^a
O ₂	Rate = $\frac{H_S \{ k_2 + k_{10} K_W / [H^+] \} K_{2S} k_3}{k_{-2} [H^+]^2 + k_{-10} [H^+] + k_{2S} k_3} P_{SO_2}$
O ₃	Rate = $\{ k_4 [HSO_3^-] + k_5 [SO_3^{-2}] \} [O_3 \cdot H_2O]$
Fe ⁺⁺⁺	Rate = $\frac{k_0 k_S^2 H_S^2 P_{SO_2}^2 [Fe^{+++}]}{[H^+]^3}$
Mn ⁺⁺	Rate = $3.67 \times 10^{-3} [X]^{-1.17} \{ [HSO_4^-] + [SO_4^{-2}] \}^2 \{ [Mn^{++}] - [X] \} x [H_2O(l)]^{-2}$
	where $X = \frac{k_1 H_S P_{SO_2} [Mn^{++}]}{k_1 \{ H_S P_{SO_2} + [H_2O(l)] [Mn^{++}] \} + 0.17}$
Black carbon	Rate = $k_6 [C_x] [O_2]^{.69} \frac{\alpha [S^{+4}]^2}{1 + \beta [S^{+4}] + \alpha [S^{+4}]^2}$
HNO ₂	Rate = $k_7 [H^+]^2 [NO_2^-] + k_8 [H^+] [NO_2^-] [HSO_3^-] + k_9 [NO_2^-] [HSO_3^-]^2$

^a [H₂O(l)] in cc/m³, concentration in moles/l, gas pressure in atm, and time in sec, k₀ = 151.69 l/mole-sec, k_S = 1.84 × 10⁻² mole/l, k₁ = 8.12 × 10⁴ l/mole-sec, k₂ = 3.4 × 10⁶ sec⁻¹, k₋₂ = 2 × 10⁸ l/mole-sec, k₁₀ = 2.9 × 10⁵ l/mole-sec, k₋₁₀ = 2.3 × 10⁻⁷ sec⁻¹, k₃ = 1.7 × 10⁻³ sec⁻¹, k₄ = 1.1 × 10⁵ l/mole-sec, k₅ = 7.4 × 10⁸ l/mole-sec, k₆ = 1.2 × 10⁻⁴ mole^{.3} · l^{.7}/g · sec, α = 1.5 × 10¹² l²/mole², β = 3.06 × 10⁶ l/mole, k₇ = 8 × 10⁵ l²/mole²-sec, k₈ = 3.8 × 10³ l²/mole²-sec, k₉ = 9 × 10⁻⁴ l²/mole²-sec.

and HNO_2) is governed by chemical reactions.

2. There is no mass transfer of any species across the box during the reaction; therefore, the SO_2 (and NH_3 or HNO_2) in each box is depleted with time. The mass balance of the SO_2 , CO_2 , NH_3 , and HNO_2 is always maintained (i.e., $\Delta[\text{SO}_2]_{\text{g}} = \Delta[\text{SO}_2 \cdot \text{H}_2\text{O}] + \Delta[\text{HSO}_3^-] + \Delta[\text{SO}_3^{-2}] + \Delta[\text{HSO}_4^-] + \Delta[\text{SO}_4^{-2}]$; $\Delta[\text{CO}_2]_{\text{g}} = \Delta[\text{CO}_2 \cdot \text{H}_2\text{O}] + \Delta[\text{HCO}_3^-] + \Delta[\text{CO}_3^{-2}]$; $\Delta[\text{NH}_3]_{\text{g}} = \Delta[\text{NH}_3 \cdot \text{H}_2\text{O}] + \Delta[\text{NH}_4^+]$; and $\Delta[\text{HNO}_2]_{\text{g}} = \Delta[\text{HNO}_2] + \Delta[\text{NO}_2^-] + 2\Delta[\text{N}_2\text{O}]_{\text{g}}$; all units are in mole).

3. The growth of liquid water droplets due to the vapor pressure lowering effect of the sulfuric acid formed in the droplets is neglected.

The rate of sulfate production is determined by a calculation scheme involving a combination of equilibrium and kinetic steps. Equilibrium between SO_2 in the gas phase and sulfur (IV) in the droplet is several orders of magnitude faster than oxidation of sulfur (IV) to sulfate (Beilke and Gravenhorst, 1978). Similar assumptions were made regarding NH_3 and CO_2 gases. Therefore, initially gases are taken to be in equilibrium with the aerosols. Then the formation of sulfate proceeds by the given time-dependent production rate. The increase in the sulfate level in the small time step Δt causes the reduction in pH of the solution, which in turn disturbs the equilibrium between the aerosol and its surrounding gaseous environment. More gases are dissolved in the aerosol to maintain the equilibrium. At the same time, these gases are depleted in the surrounding

atmosphere. After each calculation, the time step is adjusted and the process is repeated until a 24-hour period is completed. The results are shown in Figure 12.

Figure 12 indicates that O_3 , black carbon, and HNO_2 can be important mechanisms for sulfate aerosol formation. In general the O_3 mechanism is more important under high pH and/or photoactivity conditions when the concentration of O_3 is high, whereas both carbon and HNO_2 processes are more important when the lifetime of fog or clouds is long and the pH of the droplets is low. Both carbon and HNO_2 processes can be dominant processes close to sources and in heavily polluted urban areas, where the concentrations of soot and NO/NO_2 are high and the pH of aqueous droplets is low.

The rate constants for atmospheric black carbon particles varies, depending on the nature and history of particle production as discussed previously. In a fog chamber study, Benner (1980) recently found that the reaction rate of soot particles from a natural gas diffusion flame can be considerably faster than the reaction rate reported here. More determination of rate constants of soot from different types of fuel is therefore warranted.

ACKNOWLEDGMENT

This work was supported by the Assistant Secretary for the Environment, Office of Health and Environmental Research, Pollutant Characterization and Safety Division of the U.S. Department of Energy under Contract No. W-7405-ENG-48 and by the National Science

Foundation under Contract No. ATM 80-13707.

REFERENCES

- Beilke, S., Lamb, D., and Müller, J. (1975) On the uncatalyzed oxidation of atmospheric SO_2 by oxygen in an aqueous system. Atmos. Environ. 9, 1083-1090.
- Beilke, S. and Gravenhorst, G. (1978) Heterogeneous SO_2 oxidation in the droplet phases. Atmos. Environ. 12, 231-239.
- Benner, W.H. (1980) Private communication.
- Bente, P.F. and Walton, J.H. (1943) The catalytic activity of activated nitrogenous carbons. J. Phys. Chem. 47, 133-148.
- Boehm, H.P., Diehl, E., Heck, W., and Sappok, R. (1964) Surface oxides of carbon. Angew. Chem. Int. Ed. Engl. 3, 669-677.
- Boehm, H.P. (1966) Chemical identification of surface groups. Advan. Catal. Relat. Subj. 16, 179-274.
- Britton, L.G. and Clarke, A.G. (1980) Heterogeneous reactions of sulphur dioxide and SO_2/NO_2 mixtures with a carbon soot aerosol. Atmos. Environ. 14, 829-839.
- Brodzinsky, R., Chang, S.G., Markowitz, S.S., and Novakov, T. (1980) Kinetics and mechanism for the catalytic oxidation of sulfur dioxide on carbon in aqueous suspensions. J. Phys. Chem. 84, 3354-3358.

- Brosset, C. (1980) Equilibrium composition of aerosols generated from sulphuric and nitric acids, water and ammonia. Paper presented at the Chemical Institute of Canada Annual Meeting, Ottawa, Ontario, June 8-11, 1980.
- Chang, S.G. and Novakov, T. (1975) Infrared and Photoelectron Spectroscopic Study of SO₂ Oxidation on Soot Particles. Lawrence Berkeley Laboratory Report LBL-4446.
- Chang, S.G., Brodzinsky, R., Toossi, R., Markowitz, S.S., and Novakov, T. (1979). Catalytic oxidation of SO₂ on carbon in aqueous suspensions. Proc. Conference on Carbonaceous Particles in the Atmosphere, pp. 122-130. Lawrence Berkeley Laboratory Report LBL-9037.
- Chang, S.G., Toossi, R., and Novakov, T. (1981) The importance of soot particles and nitrous acid in oxidizing SO₂ in atmospheric aqueous droplets. Atmos. Environ. 15, 1287-1292.
- Clark, A. (1970) The Theory of Adsorption and Catalysis, Academic Press, New York.
- Cofer III, W.R., Schryer, D.R., and Rogowski, R.S. (1980) The enhanced oxidation of SO₂ by NO₂ on carbon particulates. Atmos. Environ. 14, 571-575.
- Cofer III, W.R., Schryer, D.R., and Rogowski, R.S. (1981) The oxidation of SO₂ on carbon particles in the presence of O₃, NO₂, and N₂O. Atmos. Environ. 15, 1281-1286.

- Coughlin R.W. and Ezra, F.S. (1968) Role of surface acidity in the adsorption of organic pollutants on the surface of carbon. Environ. Sci. Technol. 2, 291-297.
- Coughlin, R.W. (1969) Carbon as adsorbent and catalyst. I&EC Prod. Res. & Develop. 8, 12-23.
- Davtyan, O.K. and Tkach, Yu.A. (1961) The mechanism of oxidation, hydrogenation, and electrochemical oxidation on solid catalysts. II. The catalytic activity of surface "oxides" on carbon. Russian J. Phys. Chem. 35, 992-998.
- Dulou, R. (1945) Catalyse par les adsorbants non métalliques. Chim. Ind. (Paris) 54, 396-403.
- Emmett, P.H. (1948). Adsorption and pore-size measurements on charcoals and whetlerites. Chem. Rev. 43, 69-148.
- Erickson, R.E., Yates, L.M., Clark, R.L., and McEwen, D. (1977) The reaction of sulfur dioxide with ozone in water and its possible atmospheric significance. Atmos. Environ. 11, 813-817.
- Freiberg, J. (1975) The mechanism of iron catalyzed oxidation of SO₂ in oxygenated solutions. Atmos. Environ. 9, 661-673.
- Friedel, R.A. and Hofer, L.J.E. (1970). Spectral characterization of activated carbon. J. Phys. Chem. 74, 2921-2922.

- Frumkin, A., Burstein, R., and Lewin, P. (1931) Über aktivierte Kohle. Z. Phys. Chem. A157, 442-446.
- Garten, V.A. and Weiss, D.E. (1957) The ion- and electron-exchange properties of activated carbon in relation to its behaviour as a catalyst and adsorbent. Rev. Pure Appl. Chem. 7, 69-122.
- Garten, V.A., Weiss, D.F., and Willis, J.B. (1957) A new interpretation of the acidic and basic structures in carbon. I. Lactone groups of the ordinary and fluorescein types in carbon. Aust. J. Chem. 10, 295-308.
- Gordon, G.E., Davis, D.D., Israel, G.W., Landsberg, H.E., and O'Haver, T.C. (1975) Atmospheric Impact of Major Sources and Consumers of Energy. NSF/RA/E-75/189 (NTIS PB 262 574).
- Gundel, L.A. (1979) Private communication.
- Gundel, L.A., Chang, S.G., Clemenson, M.S., Markowitz, S.S., and Novakov, T. (1979) Characterization of particulate amines, in Nitrogenous Air Pollutants, Ann Arbor Science, Ann Arbor, pp. 211-220.
- Hansen, A.D.A., et al. (1980) The use of an optical attenuation technique to estimate the carbonaceous component of urban aerosols, in Atmospheric Aerosol Research Annual Report FY-1979, Lawrence Berkeley Laboratory Report LBL-10735, pp. 8-16 - 8-21.

- Hart, P.J., Vastola, F.J., and Walker, Jr., P.L. (1967) Oxygen chemisorption on well cleaned carbon surfaces. Carbon 5, 363-371.
- Hoffman, U. and Wilm, D. (1936) Über die Kristallstruktur von Kohlenstoff. Z. Elektrochem. angew. physik. Chem. 42, 504-522.
- Laine, N.R., Vastola, F.J., and Walker, Jr., P.L. (1963) The importance of active surface area in the carbon oxygen reaction. J. Phys. Chem. 67, 2030-2034.
- Larsen, E.C. and Walton, J.H. (1940) Activated carbon as a catalyst in certain oxidation-reduction reactions. J. Phys. Chem. 44, 70-85.
- Lau, N.C. and Charlson, R.J. (1977) On the discrepancy between background atmospheric ammonia gas measurements and the existence of acid sulfates as a dominant atmospheric aerosol. Atmos. Environ. 11, 475-478.
- Matteson, M.J., Stöber, W., and Luther, H. (1969) Kinetics of the oxidation of sulfur dioxide by aerosols of manganese sulfate. Ind. Eng. Chem. Fundam. 8, 677-687.
- Mattson, J.S. and Mark, Jr., H.B. (1971) Activated Carbon, Ch. 6, Marcel Dekker, New York, pp. 129-156.
- Novakov, T., Mueller, P.K., Alcocer, A.E., and Otvos, J.W. (1972) Chemical composition of Pasadena aerosol by particle size and time of day. III. Chemical states of nitrogen and sulfur by photoelectron

- spectroscopy. J. Colloid Interface Sci. 39, 225-234.
- Novakov, T. (1973) Chemical characterization of atmospheric pollution particulates by photoelectron spectroscopy. Proc, 2nd Joint Conference on Sensing of Environmental Pollutants, Instrument Society of America, Pittsburgh, pp. 197-204.
- Novakov, T., Chang, S.G., and Harker, A.B. (1974) Sulfates in pollution particulates: Catalytic oxidation of SO₂ on carbon particles. Science 186, 259-261.
- Novakov, T. and Chang, S.G. (1977) ESCA in Environmental Chemistry. Lawrence Berkeley Laboratory Report LBL-6323; to be published as a chapter in Advances in Analytical Chemistry, D. Natusch, ed., American Chemical Society.
- Novakov, T. (1981) Microchemical characterization of aerosols, in H. Malissa, M. Grasserbauer, and R. Belcher, Eds., Nature, Aim and Methods of Microchemistry, Springer-Verlag, Vienna, pp. 141-165.
- Oblath, S.B., Markowitz, S.S., Novakov, T., and Chang, S.G. (1980) Kinetics of the formation of hydroxylamine disulfonate by reaction of nitrite with sulfites. J. Phys. Chem. 85, 1017-1021.
- Palmer, H.B. and Cullis, C.F. (1965) The formation of carbon from gases, in Chemistry and Physics of Carbon, Vol. I, Dekker, New York, pp. 265-325.

- Puri, B.R. (1962) Surface oxidation of charcoal at ordinary temperatures. Proc. Conference on Carbon, 5th, Vol. I, Pergamon Press, Oxford, pp. 165-170.
- Puri, B.R. (1966) Chemisorbed oxygen evolved as carbon dioxide and its influence on surface reactivity of carbons. Carbon 4, 391-400.
- Puri, B.R. (1970) Surface complexes on carbon, in Chemistry and Physics of Carbon, Vol. VI, Dekker, New York, pp. 191-282.
- Rao, M.N. and Hougen, O.H. (1952) Catalytic oxidation of nitric oxide on activated carbon. Chem. Eng. Progr. Symp. Series 48, 110-124.
- Rivin, D. (1963) Hydride-transfer reactions of carbon black. Proc. Conference on Carbon, 5th, Vol. II, Pergamon Press, Oxford, pp. 199-209.
- Rosen, H., Hansen, A.D.A., Gundel, L., and Novakov, T. (1978) Identification of the optically absorbing component of urban aerosols. Appl. Opt. 17, 3859-3861.
- Rosen, H., Hansen, A.D.A., Dod, R.L., and Novakov, T. (1980) Soot in urban atmospheres: Determination by an optical absorption technique. Science 208, 741-744.
- Rosen, H., Novakov, T., and Bodhaine, B.A. (1981) Soot in the Arctic. Atmos. Environ. 15, 1371-1374.
- Schilow, N., Schatunowskja, H., and Tschmutow, K. (1930) Adsorptionsercheinungen in Lösungen. XX. Über den chemischen

- Zustand der Oberfläche von aktiver Kohle. Z. Phys. Chem. (Leipzig) A149, 211-222.
- Siedlewski, J. (1965) The mechanism of catalytic oxidation on activated carbon: The influence of free carbon radicals on the adsorption of SO₂. Int. Chem. Eng. 5, 297-301.
- Smith, R.N. (1959) The chemistry of carbon-oxygen surface compounds. Quarterly Rev. 13, 287-305.
- Steenberg, B. (1944) Adsorption and Exchange of Ions on Activated Charcoal, Almqvist and Wiksells, Uppsala.
- Stumpp, E. (1965) Untersuchungen über den Ameisensäurezerfall an Graphit und an Metallchlorid-Graphitverbindungen. Z. anorg. allgem. Chem. 337, 292-300.
- Tuinstra, F. and Koenig, J.L. (1970) Raman spectrum of graphite. J. Chem. Phys. 53, 1126-1130.
- Weller, S.W. and Young, T.F. (1948) Oxygen complexes on charcoal. J. Am. Chem. Soc. 70, 4155-4162.
- Yamamoto, K., Seki, M., and Kawazoe, K. (1972) Absorption of sulfur dioxide on activated carbon in the flue gas desulfurization process. III. Rate of oxidation of sulfur dioxide on activated carbon surfaces. Nippon Kagaku Kaishi 6, 1046-1052.

Yasa, Z., Amer, N., Rosen, H., Hansen, A.D.A., and Novakov, T. (1978)
Photoacoustic investigation of urban aerosol particles. Appl. Opt.
18, 2528-2530.

Zarifyanz, Y.A., Kiselev, V.F., Lezhnev, N.N., and Nikitina, D.V.
(1967) Interaction of graphite fresh surface with different gases
and vapors. Carbon 5, 127-135.

FIGURE CAPTIONS

Figure 1. Oxygen-containing functional groups on elemental carbon particle surfaces.

Figure 2. Nitrogen (1s) ESCA spectrum of cold soot particles exposed to NH_3 . The setup used for exposure is also shown.

Figure 3. Nitrogen (1s) ESCA spectrum of hot soot particles exposed to NH_3 . The experimental arrangement used for sample preparation is also shown.

Figure 4. Nitrogen (1s) ESCA spectrum of an ambient sample as measured at 25, 80, 150, 250, and 350°C.

Figure 5. Nitrogen (1s) spectrum of (hot) soot sample exposed to NH_3 , as measured at 25, 150, 250, and 350°C.

Figure 6. Infrared spectra of the graphite particles after extensive grinding in an atmosphere of NH_3 (a) and ND_3 (c). (b) and (d) are 2X expansions along the ordinate of (a) and (c) respectively.

Figure 7. S(IV) concentration as a function of time for acetylene and natural gas soot suspensions.

Figure 8. S(IV) and SO_4^{-2} concentrations as a function of time for a 0.16%-by-weight activated carbon suspension.

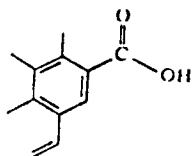
Figure 9. Effective rate of oxidation of S(IV) catalyzed on various activated carbon particles vs. S(IV) concentration.

Figure 10. The effect of the pH of aqueous droplets on $f[\text{S(IV)}]$ at $P_{\text{SO}_2} = 100, 10, \text{ and } 1$ ppb. $f[\text{S(IV)}]$ is a function of S(IV) that the aqueous oxidation rate of sulfites on soot particles depends on.

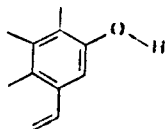
Figure 11. The effect of partial pressure of SO_2 on $f[\text{S(IV)}]$ at pH of 7, 6, 5, 4, and 3. $f[\text{S(IV)}]$ is a function of S(IV) that the aqueous oxidation rate of sulfites on soot particles depends on.

Figure 12. Comparison of the relative importance of various sulfate production mechanisms involving liquid water based on a box-type calculation. The following initial conditions were used

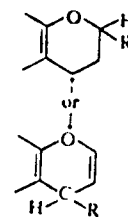
in the calculation: $P_{\text{SO}_2} = 0.01$ ppm; $P_{\text{CO}_2} = 0.000311$ atm; $P_{\text{NH}_3} = 5$ ppb; $P_{\text{O}_3} = 0.05$ ppm; $P_{\text{HNO}_2} = 8$ ppb; $[\text{Fe}^{+++}] = 1.2 \times 10^{-7}$ mole/l; $[\text{Mn}^{++}] = 1.8 \times 10^{-8}$ mole/l; soot = $10 \mu\text{g}/\text{m}^3$; and liquid water = $0.05 \text{ g}/\text{m}^3$.



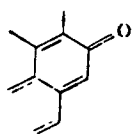
carboxyl groups



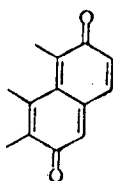
phenolic hydroxyl groups



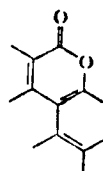
ethers (chromene)



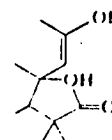
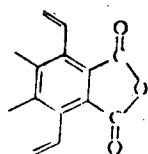
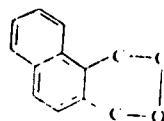
carboxyl groups



quinones



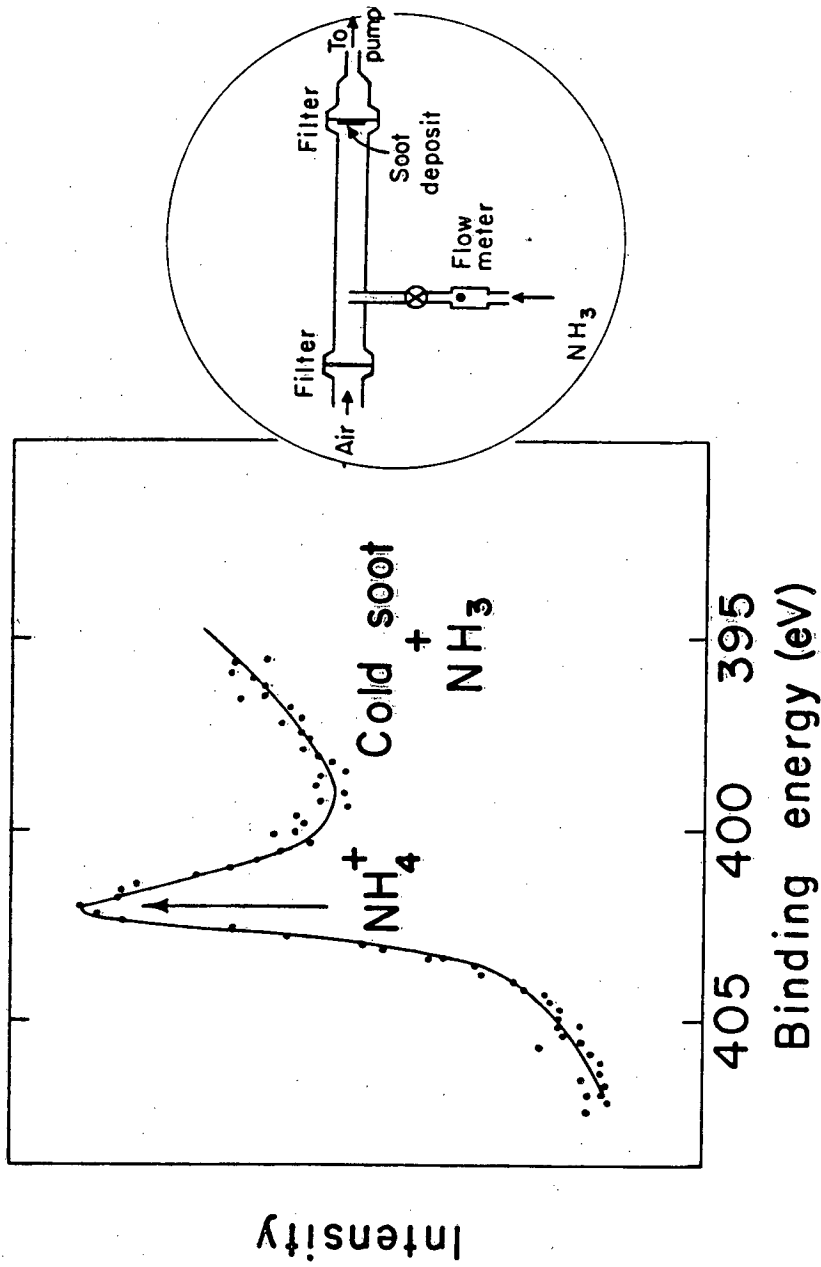
lactones

fluorescein-like
lactonescarboxylic acid
anhydrides

cyclic peroxide

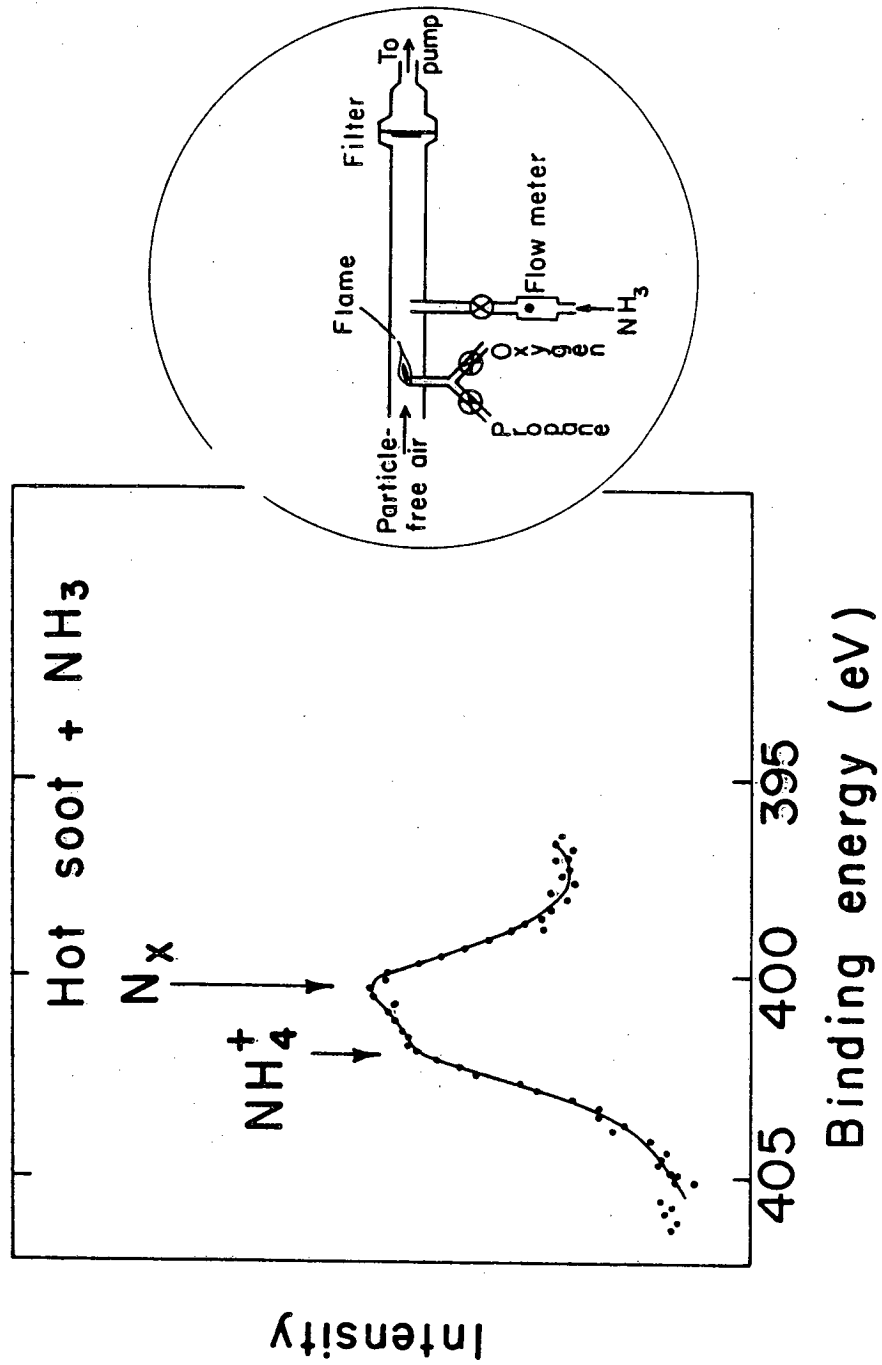
XBL 8010-12445

Figure 1



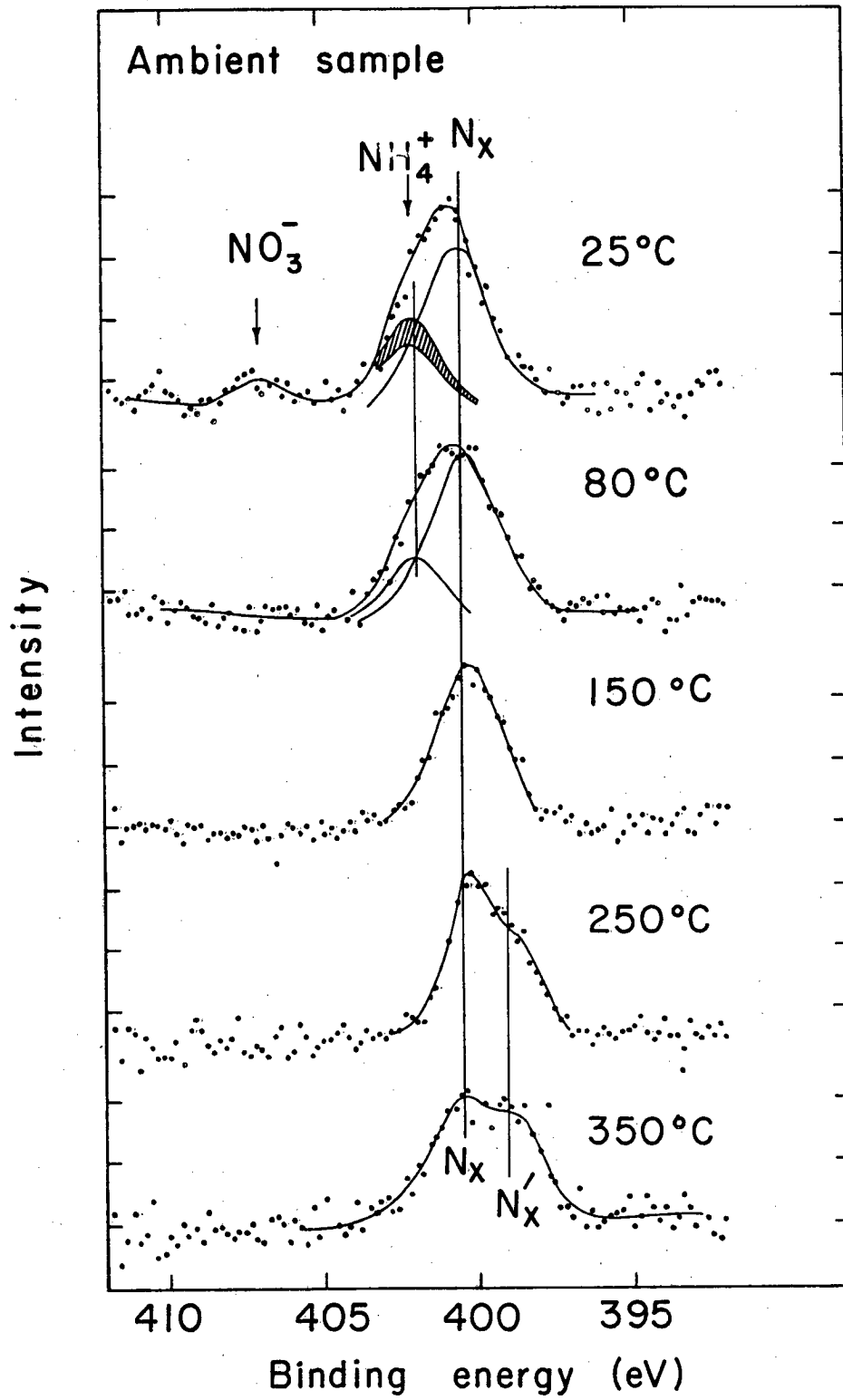
XBL 8010-12443

Figure 2



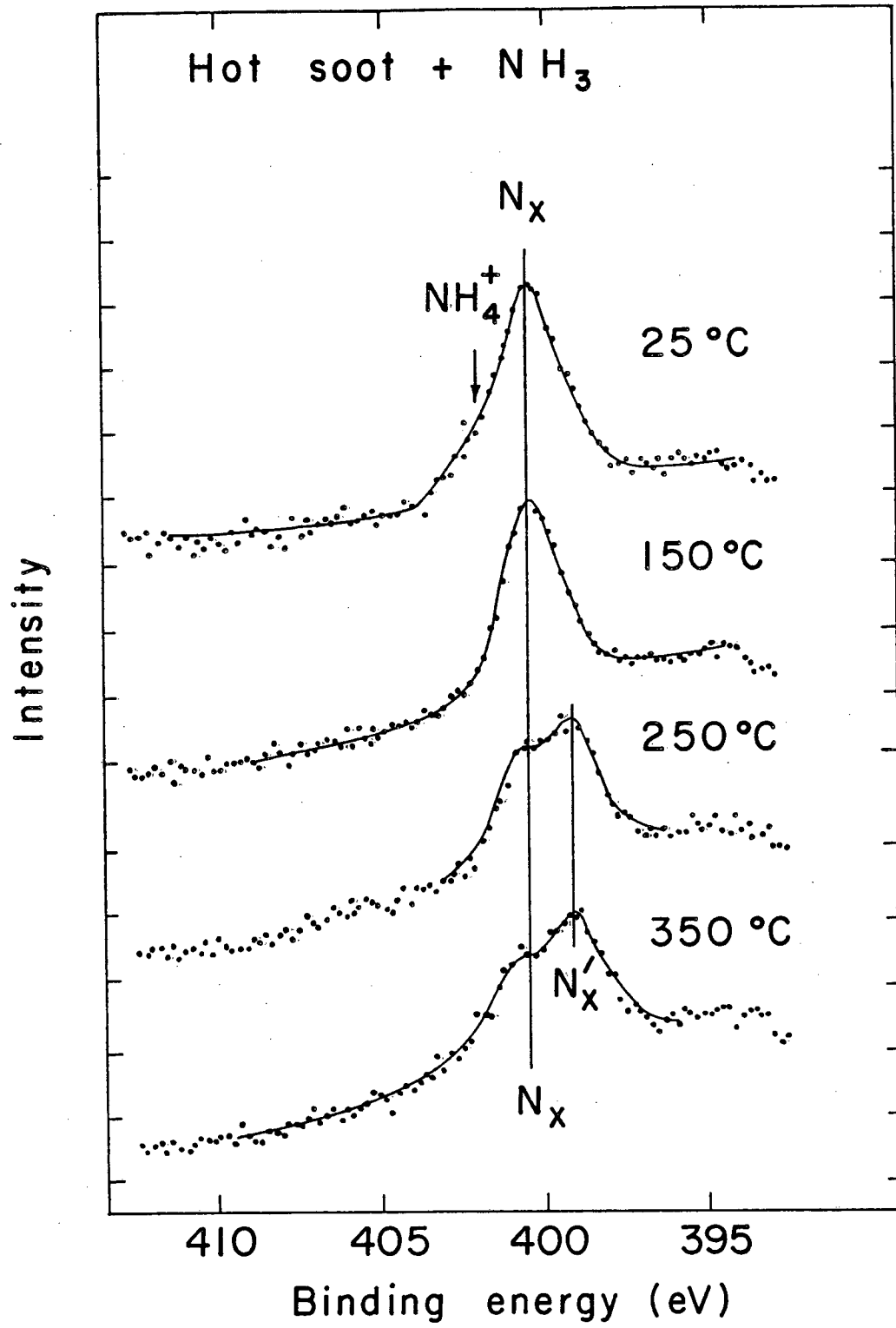
XBL 8010-12441

Figure 4



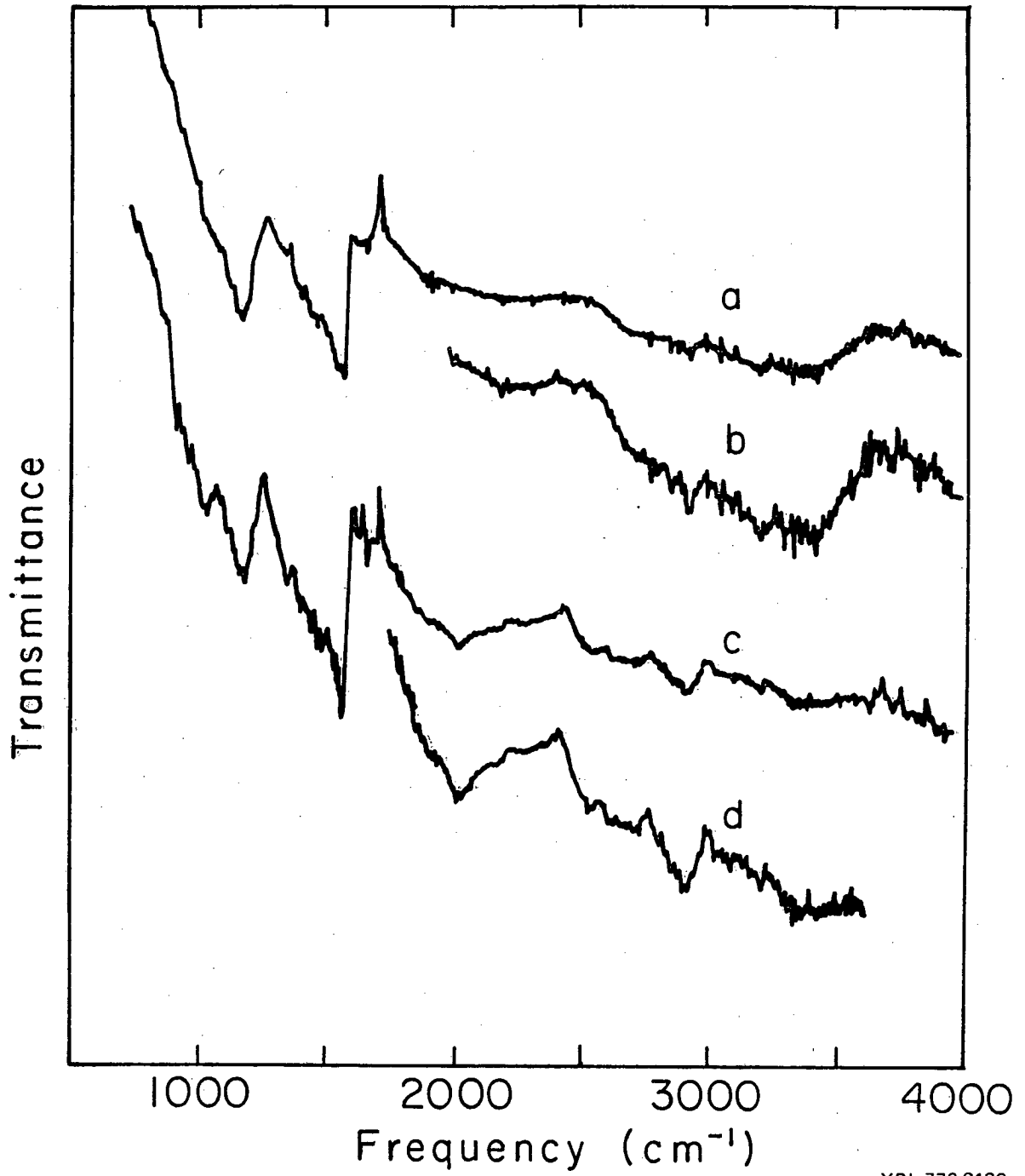
XBL746-3532

Figure 5



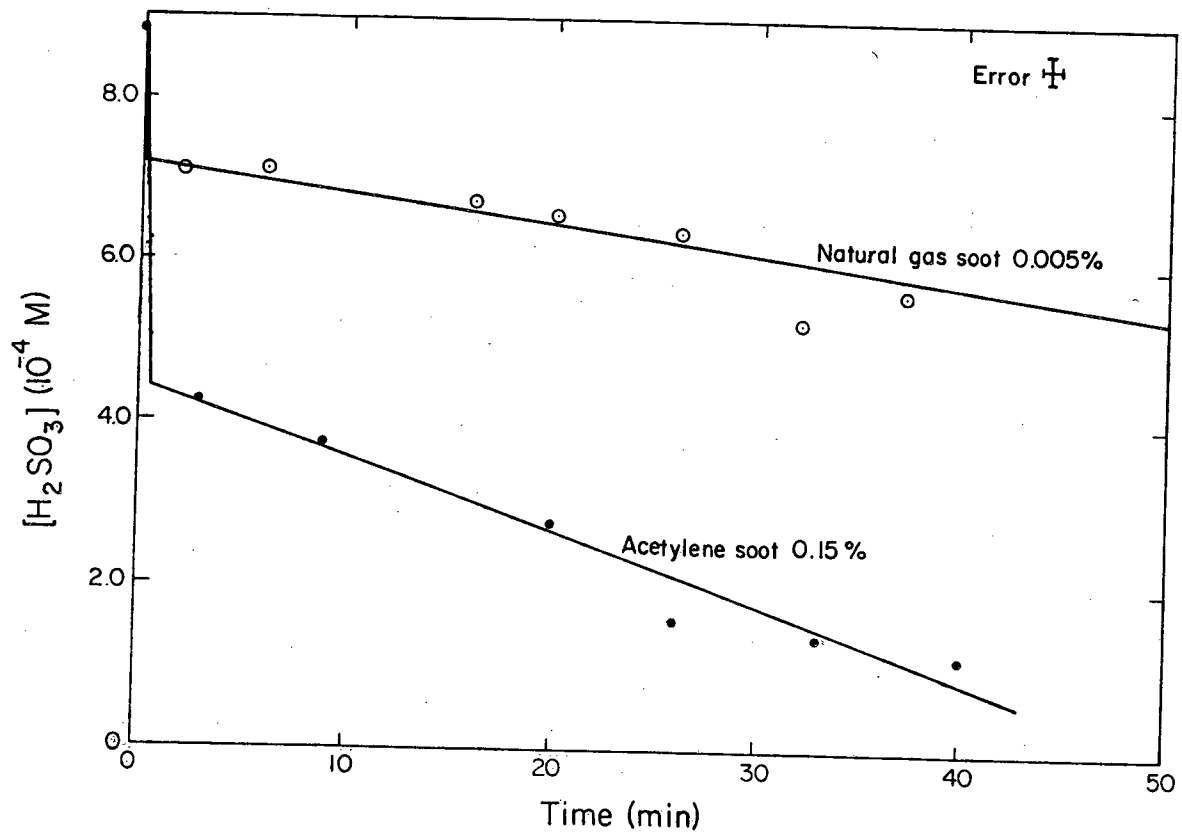
XBL746-3531

Figure 6



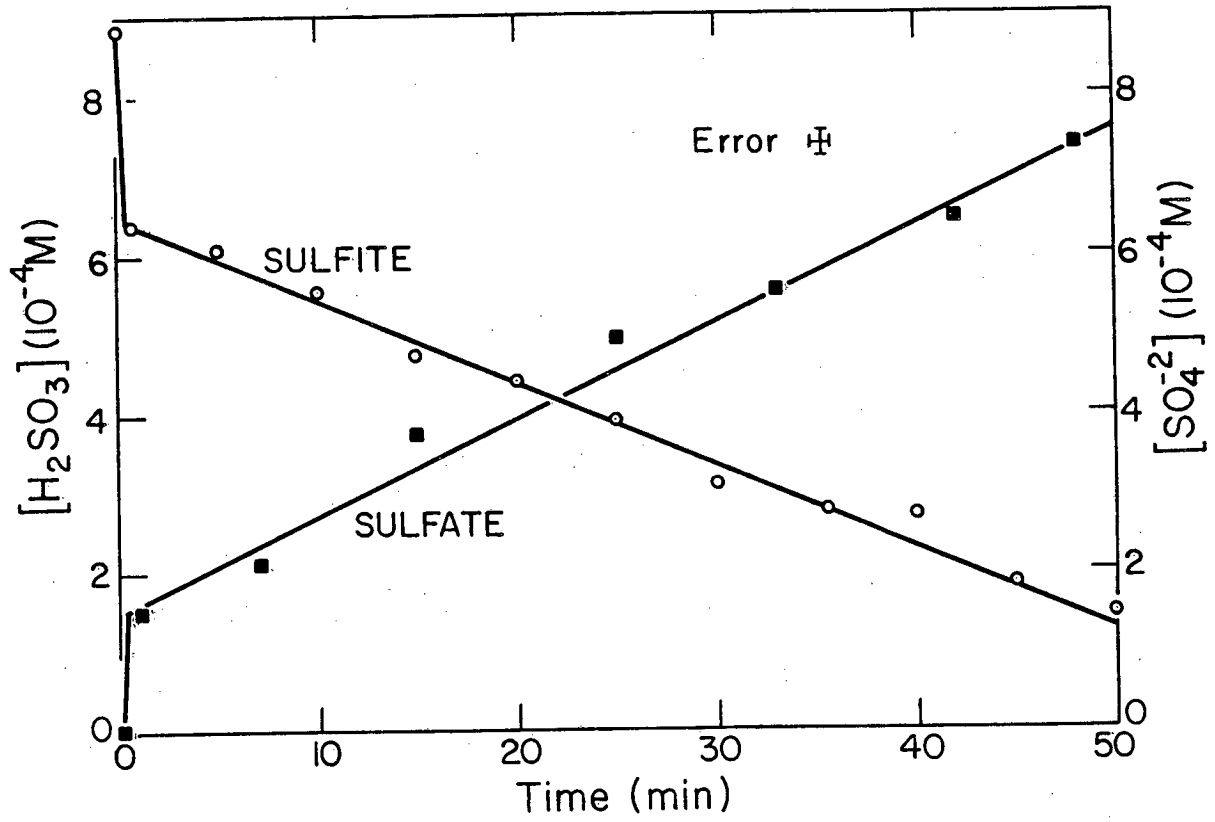
XBL 773-8123

Figure 7



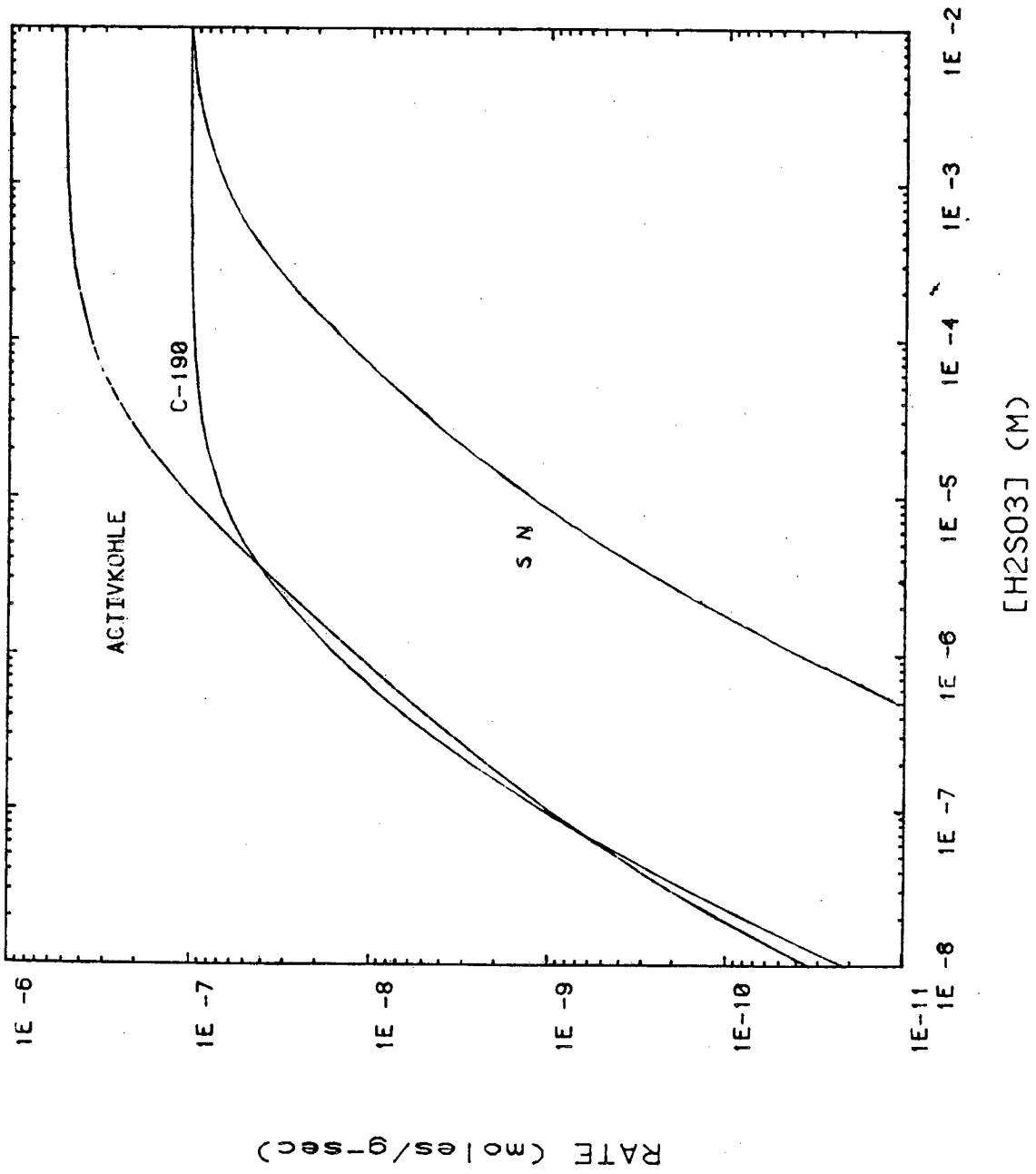
XBL7710-2065A

Figure 8



XBL 782-219

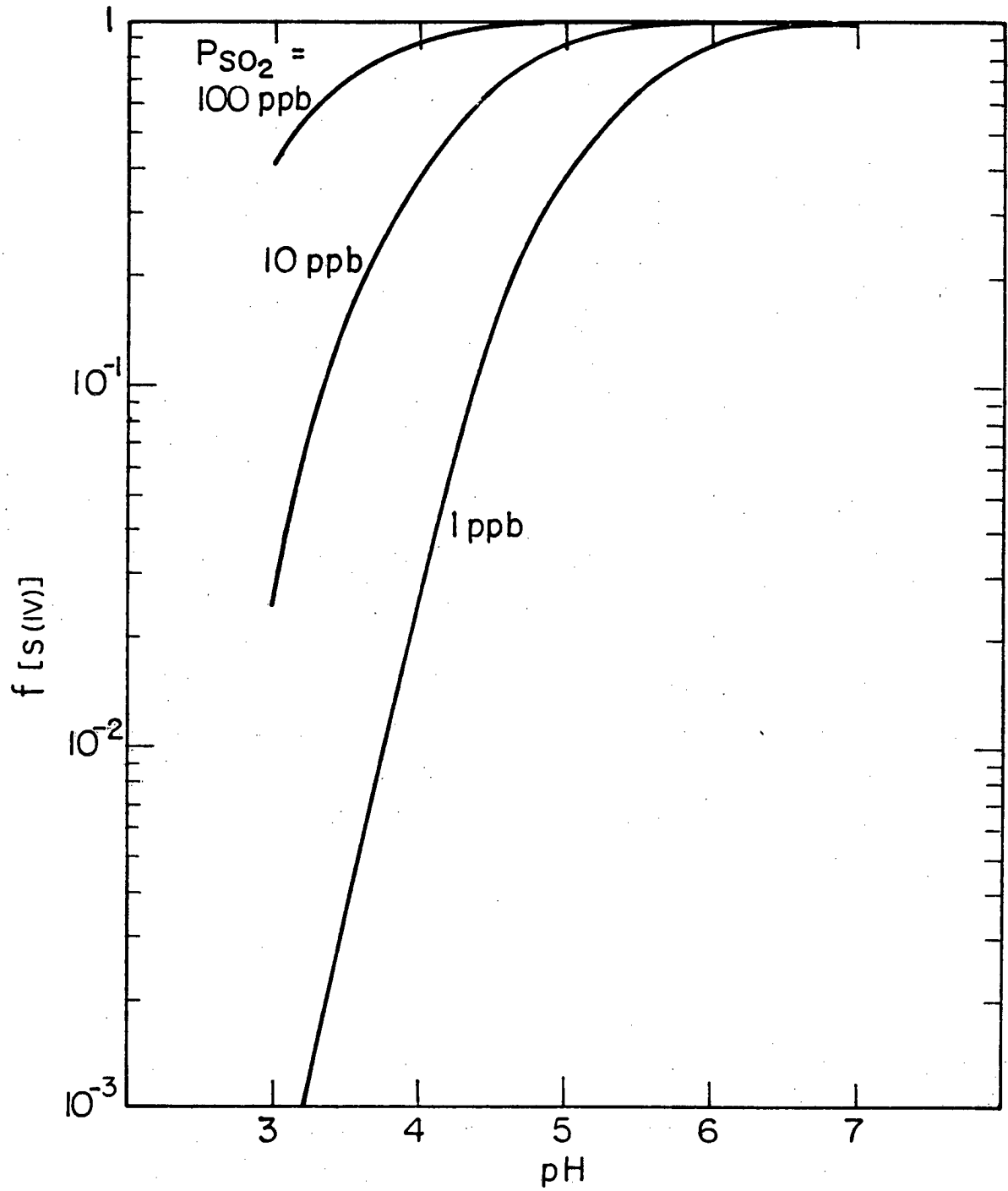
Figure 9



XBL 8010-12442

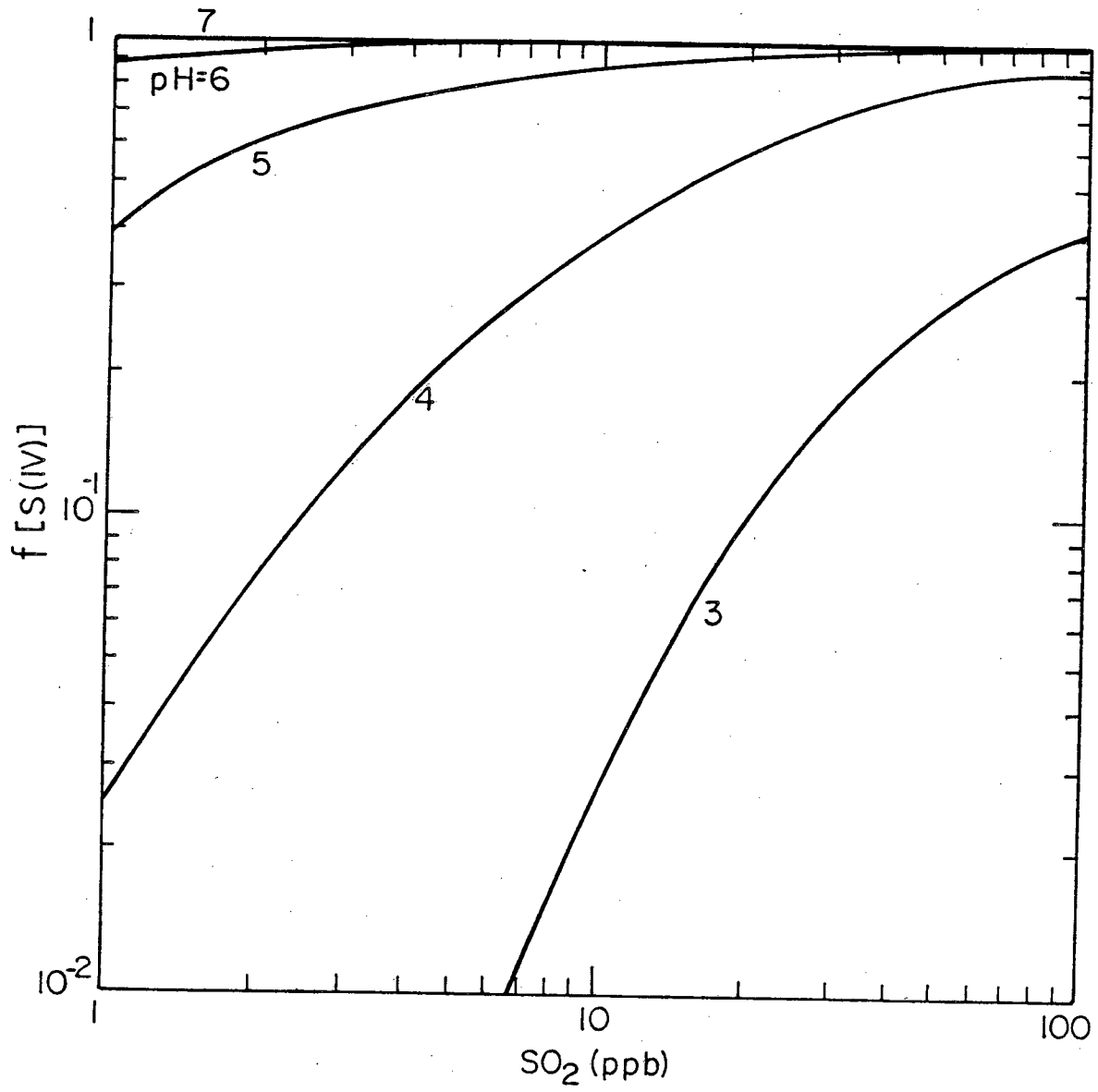
Figure 10

5. 1. 2



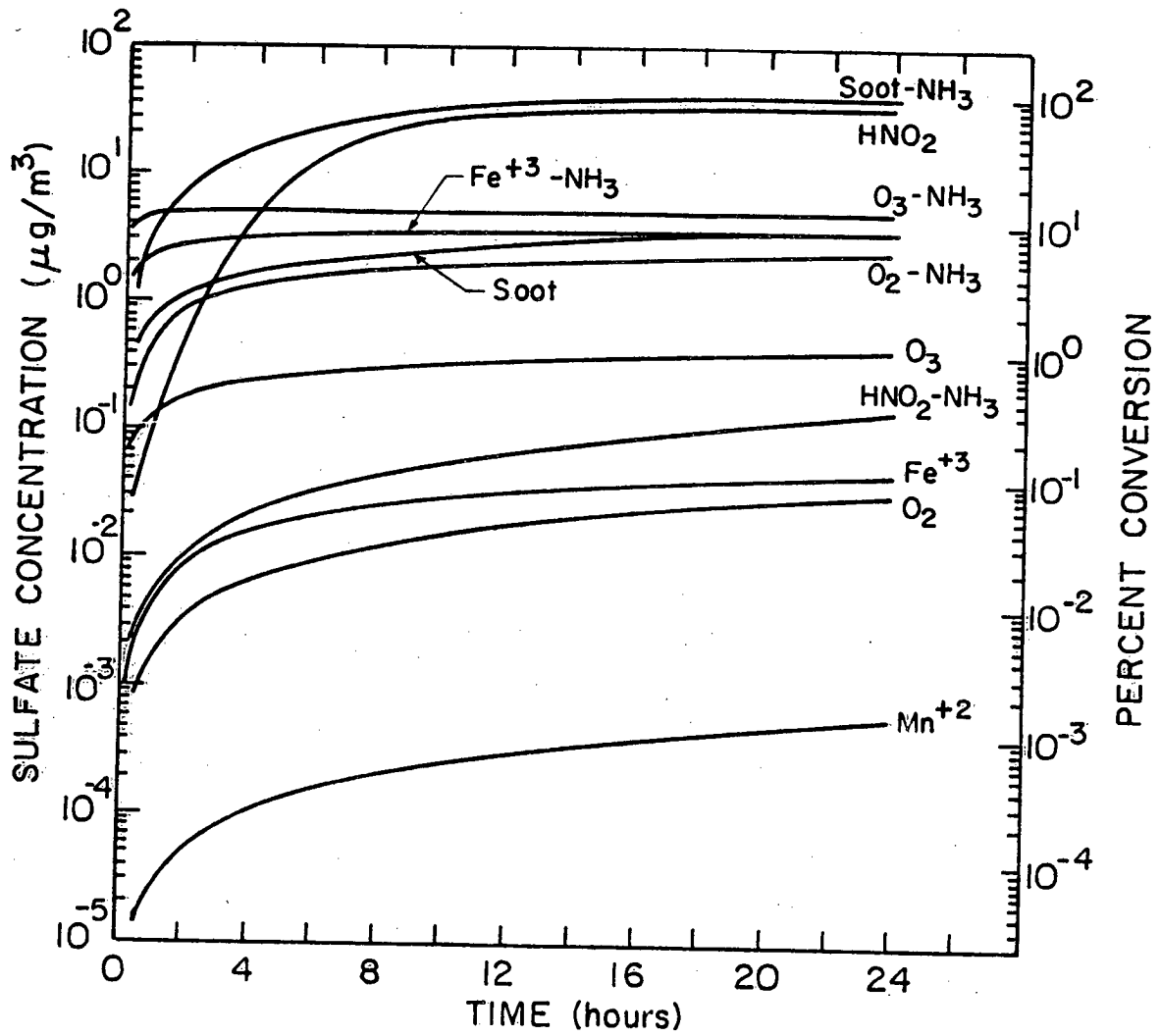
XBL808-5732

Figure 11



XBL 808-5733

Figure 12



XBL808-5735

Figure 13

This report was done with support from the Department of Energy. Any conclusions or opinions expressed in this report represent solely those of the author(s) and not necessarily those of The Regents of the University of California, the Lawrence Berkeley Laboratory or the Department of Energy.

Reference to a company or product name does not imply approval or recommendation of the product by the University of California or the U.S. Department of Energy to the exclusion of others that may be suitable.

TECHNICAL INFORMATION DEPARTMENT
LAWRENCE BERKELEY LABORATORY
UNIVERSITY OF CALIFORNIA
BERKELEY, CALIFORNIA 94720